AD-A149 827 BOUNDARY ELEMENTS FOR DEBOND STRESS ANALYSIS; FRACTURE MECHANICS STRESS A..(U) IMPERIAL COLL OF SCIENCE AND TECHNOLOGY LONDON (ENGLAND) DEPT.. C ATKINSON 1/1

UNCLASSIFIED 26 APR 83 AFOSR-TR-84-1207 AFOSR-82-0131 F/G 12/1 NL

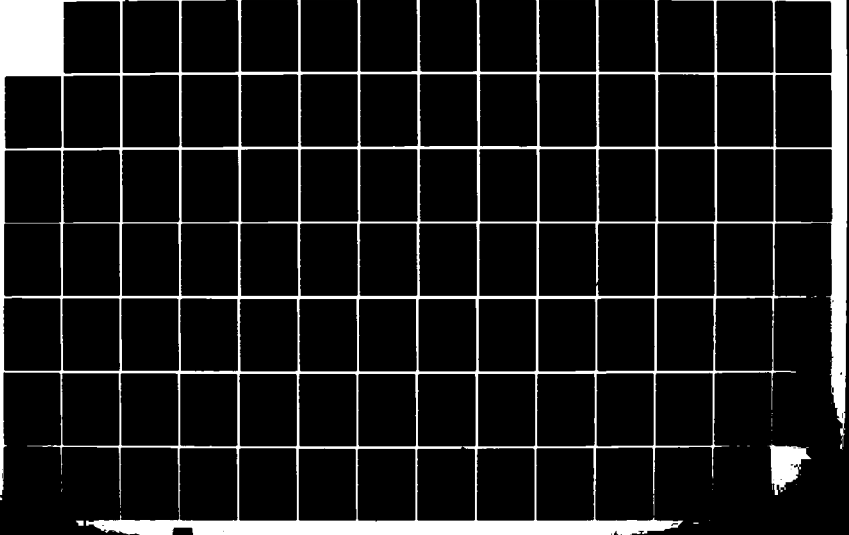

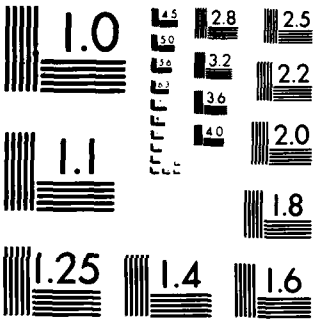

AD-A149 827

DTIC FILE COPY

REPORT DOCUMENTATION PAGE	READ INSTRUCTIONS BEFORE COMPLETING FORM
1. REPORT NUMBER: AFOSR-TR- 84-1207	2. GOVT ACCESSION NO. / 3. RECIPIENT'S CATALOG NUMBER
4. TITLE: BOUNDARY ELEMENTS FOR DEBOND STRESS ANALYSIS; Fracture mechanics stress analysis	5. TYPE OF REPORT & PERIOD COVERED: FINAL 01 MAR 82-28 FEB 83 / 6. PERFORMING ORG. REPORT NUMBER
7. AUTHOR(s): COLIN ATKINSON	8. CONTRACT OR GRANT NUMBER(s): AFOSR-82-0131
9. PERFORMING ORGANIZATION NAME AND ADDRESS: IMPERIAL COLLEGE OF SCIENCE & TECHNOLOGY LONDON SW7 2BZ : UNITED KINGDOM	10. PROGRAM ELEMENT, PROJECT, TASK AREA & WORK UNIT NUMBERS: 61102F 2307/B2
11. CONTROLLING OFFICE NAME AND ADDRESS: EOARD Box 14 FPO NY 09510	12. REPORT DATE: 26th APRIL 1983 / 13. NUMBER OF PAGES: 81
14. MONITORING AGENCY NAME & ADDRESS (if different from Controlling Office): Air Force Office of Scientific Research/NA Bolling AFB DC 20332-6600	15. SECURITY CLASS. (of this report): UNCLASSIFIED / 15a. DECLASSIFICATION DOWNGRADING SCHEDULE

16. DISTRIBUTION STATEMENT (of this Report)

Approved for public release; distribution unlimited.

17. DISTRIBUTION STATEMENT (of the abstract entered in Block 20, if different from Report)

18. SUPPLEMENTARY NOTES

19. KEY WORDS (Continue on reverse side if necessary and identify by block number)

BOUNDARY INTEGRAL EQUATIONS
BOUNDARY ELEMENTS
BOUNDARY ELEMENT METHODS
FRACTURE MECHANICS
STRESS SINGULARITIES

20. ABSTRACT (Continue on reverse side if necessary and identify by block number)

To understand and quantify debonding events in composite materials it is necessary to have accurate stress analysis in the area of stress concentrators. Boundary integral equation (BIE) techniques are proposed as a potentially more accurate approach than finite elements. In particular, the debond stress analysis of a rod being pulled out of a matrix material is considered. A model problem is posed consisting of an edge cracked bar under longitudinal shear deformation and a BIE formulation is proposed using a subtraction

DD FORM 1 JAN 73 1473 EDITION OF 1 NOV 65 IS OBSOLETE

UNCLASSIFIED

SECURITY CLASSIFICATION OF THIS PAGE (When Data Entered)

20. (Cont.)

of singularity technique. An extensive review of integral equation approaches to various fracture mechanics problems is also presented, with suggested new solution techniques for unsymmetric crack configurations.

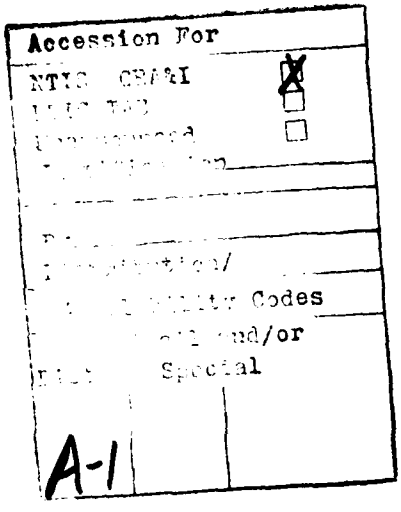

AFOSR-TR- 84-1207

Contract/Grant No: AFOSR - 82 - 0131

BOUNDARY ELEMENTS FOR DEBOND STRESS ANALYSIS: Fracture Mechanics Stress Analysis

Colin Atkinson
Department of Mathematics
Imperial College of Science & Technology
LONDON SW7 2BZ

26th April 1983

Final Report, 1st March 1982 - 28th February 1983

Prepared for: UNITED STATES AIR FORCE
Air Force Office of Scientific Research
Building 410, Bolling AFB, D.C. 20332

and EUROPEAN OFFICE OF AEROSPACE RESEARCH
AND DEVELOPMENT
London, England.

1. INTRODUCTION

In order to understand and quantify debonding events in composite materials under stress it is necessary to have accurate stress analysis in the vicinity of stress concentrators. In recent work [1] the debond stress analysis of a rod being pulled out of a Solithane matrix was considered. The methods used for the stress analysis were (i) finite element calculations of the energy release rate associated with the debonding process and (ii) special analytical solutions valid for short crack initiation at key geometrical features of the rod-matrix geometry. In this second approach (which is potentially the most accurate) a key ingredient is the stress field at geometrical discontinuities lying on the rod-matrix interface. The finite element method yields very inaccurate results at such discontinuities unless special elements are used.

A popular alternative to the finite element method is the Boundary Integral Equation (B.I.E) method but it too may require special attention to the stress singularities at geometrical discontinuities. In the papers [2] and [3] a comparison of various methods of dealing with crack tip stress singularities was made for the solution of a model problem by the boundary integral equation method. The main purpose of the project reported here was to extend this work to other stress singularities by considering the model problem discussed below. A secondary objective was to attempt to develop a theory to extend the BIE applicability to unsymmetric crack configurations. Some progress on this latter objective has been made and a possible method is suggested in the Appendix where an extensive review of integral equation approaches to various fracture

mechanics problems is also presented. In our original proposal we suggested the model problem discussed below noting that experience gained from treating this simpler problem is potentially readily transferable to the elastic situation.

2. Model Problem (longitudinal shear deformation)

The normal stress σ_{nz} is assumed zero on all boundaries except the top and bottom of the slab (Fig.1) for which we assume fixed displacement loading

$$\begin{aligned} u_3 &= u_{30} \quad y = 1 \\ u_3 &= -u_{30} \quad y = -1 \end{aligned} \tag{2.1}$$

Because of the longitudinal shear (anti-plane strain) assumption the only non-zero stresses are

$$\begin{aligned} \sigma_{xz} &= \mu \frac{\partial u_3}{\partial x} \\ \sigma_{yz} &= \mu \frac{\partial u_3}{\partial y} \end{aligned} \tag{2.2}$$

and the associated equilibrium equation reduces to

$$\frac{\partial}{\partial x}\left(\mu \frac{\partial u_3}{\partial y}\right) + \frac{\partial}{\partial y}\left(\mu \frac{\partial u_3}{\partial y}\right) = 0 \tag{2.3}$$

Before considering the BIE implementation of the problem it is useful to investigate the kind of singularity which exists at notch tip A in terms of the internal angle, 2α, of the notch. Expanding the displacement field in terms of a local co-ordinate system (r,ϑ) based on the notch tip A gives

$$u_3 \sim r^{\lambda}(A_1 \cos\lambda\vartheta + B_1 \sin\lambda\vartheta) \tag{2.4}$$

as the dominant term of the notch tip $0 < \lambda < 1$. Note that this expression for u_3 is an <u>exact</u> solution of the field equation above, although it does not have the capability, of course, of satisfying all the boundary conditions of the problem. Nevertheless, the conditions on the notch sides are satisfied exactly if

$$\frac{1}{r}\frac{\partial u_3}{\partial \vartheta} = 0 \quad \text{on} \quad \vartheta = \alpha, \quad 2\pi - \alpha \tag{2.5}$$

and hence we require

$$\begin{aligned} -A_1 \sin\lambda\alpha + B_1 \cos\lambda\alpha &= 0 \\ -A_1 \sin \lambda(2\pi-\alpha) + B_1 \cos\lambda(2\pi-\alpha) &= 0 \end{aligned} \tag{2.6}$$

which is possible provided

$$\sin\lambda\alpha \cos\lambda(2\pi-\alpha) = \sin\lambda(2\pi-\alpha)\cos\lambda\alpha \qquad (2.7)$$

i.e. $\sin\lambda(2\pi-2\alpha) = 0.$

Thus $\lambda(\pi-\alpha)= \pi/2$ gives the dominant singularity. It is precisely singularities of this more general kind which occur at geometric discontinuities of rigid fibres in composite materials.

From the above analysis we expect that in the vicinity of the notch tip (A of Fig.1) the dominant part of the displacement u_3 takes the form

$$u_3 = B_0 r^{\lambda} \cos\left(\frac{\pi}{2} \frac{(\vartheta-\alpha)}{(\pi-\alpha)}\right) \qquad (2.8)$$

where $\lambda = \pi/2(\pi-\alpha),$ (2.9)

and the constant B_0 is to be determined from a full numerical analysis of the problem. It is worth noting, for later use, that expression (2.8) with λ replaced by $-\lambda$ also satisfies equation (2.3) and the boundary conditions (2.5). Although the behaviour of this solution near $r = 0$ gives infinite values for u_3 so the corresponding solution is non-physical, it is nevertheless useful in deriving the physical solution as we shall see later.

3. The boundary integral equation method

The starting point is the boundary integral equation

$$\oint T(\underline{X},\underline{Y})[u(\underline{Y})-u(\underline{X})]ds_y = \oint U(\underline{X},\underline{Y}) \frac{\partial u(\underline{Y})}{\partial N}ds_y \qquad \forall \underline{X} \in \partial\Omega \qquad (3.1)$$

where

$$U(\underline{X},\underline{Y}) \equiv \left(\frac{1}{2\pi}\right) \ln(1/r) \qquad \text{with} \quad r = |\underline{Y}-\underline{X}| \tag{3.2}$$

$\partial\Omega$ is the boundary of Ω a bounded open region in R^2.

$$T(\underline{X},\underline{Y}) \equiv \nabla_y U(\underline{X},\underline{Y}).\underline{N}(\underline{Y}) \tag{3.3}$$

where $\underline{N}(\underline{Y})$ is the outward unit normal at the point $\underline{Y} \in \partial\Omega$.
In equation (3.1)

$$\oint f(\underline{X},\underline{Y})ds_y \equiv \lim_{\epsilon \to 0} \int_{\partial\Omega \cap \partial\Omega(\underline{X},\epsilon)} f(\underline{X},\underline{Y})ds_y \tag{3.4}$$

and the region $\Omega(\underline{X},\epsilon)$ is similar to Ω but excluding a region of radius ϵ centred on the point $\underline{X}$. The function u satisfies

$$\begin{aligned} \nabla^2 u &= 0 \quad \text{in} \quad \Omega \\ u &= \bar{u} \quad \text{on} \quad \partial\Omega_1 \\ \frac{\partial u}{\partial N} &= \bar{t} \quad \text{on} \quad \partial\Omega_2 \end{aligned} \tag{3.5}$$

with $\partial\Omega = \partial\Omega_1 \cup \partial\Omega_2$.

The problem is thus to compute approximations $\tilde{u}$ and $\tilde{t}$ to u and t on $\partial\Omega_2$ and $\partial\Omega_1$ respectively from the integral equation (3.1) and boundary conditions (3.5).

Any particular boundary element method is characterised by: (a) the choice of the classes of functions used to approximate u and t and (b) the way in which the integral equation (3.1) is used in the determination of $\tilde{u}$ and $\tilde{t}$. Approximating u and t (= $\partial u/\partial N$) by linear combinations of computationally convenient functions $v_\ell^{(u)}$,

$\ell = 1,\ldots,N_1$ and $v_{\ell'}^{(t)}$, $\ell' = 1,\ldots,N_2$ respectively gives

$$\tilde{u} = \sum_{\ell=1}^{N_1} u_\ell v_\ell^{(u)} , \qquad \tilde{t} = \sum_{\ell'=1}^{N_2} t_{\ell'} v_{\ell'}^{(t)} \tag{3.6}$$

This is discussed more fully in section 4 of the appendix where an application to a cracked body is considered.

To extend these methods to notches such as that shown in Fig.1 we have considered the following three methods.

Method 1. Attempt to position nodes on the element closest to notch tip A so as to simulate the correct displacement behaviour on the notch. From equation (2.4) it follows that the required displacement behaviour is

$$\tilde{u} \sim r^{\lambda} \qquad \text{where} \quad \lambda = \frac{\pi}{2(\pi - \alpha)}$$

when $\alpha = 0$, the notch becomes a crack, $\lambda = \frac{1}{2}$ and this case is considered in section 4.2.3 of the appendix by the use of a quarter point node and quadratic elements. Our initial investigations of the case $\lambda \neq \frac{1}{2}$ suggest that this approach will work only for special values of λ e.g. if $\lambda = 1/3$ cubic elements would probably be necessary. We have not therefore pursued this avenue further but note that some work on this approach to finite elements exists see (e.g. Wait [4]).

Method 2. Subtraction of singularity technique. Extending the argument given in section 2 in deriving the dominant term for u_3 near the notich tip one can write

$$u_3 = \sum_{i=0}^{M} B_i \, r^{\lambda_i} \cos(\lambda_i(\vartheta-\alpha)) \tag{3.7}$$

where $\lambda_i = \dfrac{(2i+1)\pi}{2(\pi-\alpha)}$.

In this method expression (3.7) is subtracted from the problem before the B.I.E. solution procedure is implemented. Additional equations for the unknown coefficients B_i can be determined by imposing the boundary condition on u_3 at additional points on AC (see Fig.1). On AC the boundary conditions $u_3 = 0$ follows from symmetry, the numerical solution of the integral equation being effected on the boundary ACDEF. This method has been used effectively for a crack problem discussed in the Appendix. The problem of a re-entrant corner with interior angle $3\pi/2$ has been calculated by this method and good agreement obtained with results obtained by numerical conformal mapping (Papamichael and Whiteman [5]). A method similar to that suggested here has also been considered by Symm [6]. At present we feel that this method is potentially the most accurate for dealing with stress singularities but it is useful to calculate the coefficient B_0 of the leading term of (3.7) by an alternative method as a means of comparison.

Method 3. Evaluation of sharp notch stress concentration factors by means of a reciprocal theorem.

In section 2 of the Appendix methods are discussed for the evaluation of stress intensity factors by the use of certain invariant integrals evaluated far from the crack tip. The only one of these methods that is applicable to the sharp notch problem discussed in section 2 when $\alpha \neq 0$ is that based on Betti's reciprocal theorem given in section 2.2 of the appendix.

For the model problem of section 2 this can be written

$$\int_S \mu\hat{u} \frac{\partial u}{\partial N} ds = \int_S \mu u \frac{\partial \hat{u}}{\partial N} ds \qquad (3.8)$$

where $u = u_3$ and $\hat{u}$ satisfy equation (2.3) and S is envisaged as a closed contour such as shown dotted in Fig.1. The divergence theorem and equation (2.3) can be used to prove equation (3.8).

If for $\hat{u}$ we choose the solution

$$\hat{u} = r^{-\lambda_0} \cos(\lambda_0(\vartheta-\alpha)) \qquad (3.9)$$

with $\lambda_0 = \frac{\pi}{2(\pi-\alpha)}$, then the integrals in equation (3.8) are zero when taken along the notch sides Af and AF_1 because of the boundary conditions $\partial u/\partial N = 0$ on them. The integral around an infinitesimal loop enclosing the notch tip is proportional to the unknown coefficient B_0 on account of the dominant behaviour of the displacement field $u \equiv u_3$ there (i.e. $u_3 \sim B_0 r^{\lambda_0} \cos(\lambda_0(\vartheta-\alpha))$, for small r see equation (2.8)). Thus the coefficient B_0 can be determined from the integrals (3.8) evaluated on a contour far from the notch tip e.g. on the outer boundary FEDC $D_1E_1F_1$, the values of u and $\partial u/\partial N$ being evaluated there by a B.I.E. method.

4. Concluding remarks

We believe that method 2 discussed in section 3 is the most effective way of computing the stresses near a sharp notch tip if simple elements are used to model the boundary. If higher order elements are used more accurate results could presumably be obtained for special

cases with accurate element modelling of the displacement field at the notch. More work is required to make an extensive comparison of all possibilities, however, at present we recommend method 2 together with use of the reciprocal theorem as outlined in method 3.

References

[1] Atkinson, C., Avila, J., Betz, E. and Smelser, R.E. (1982). The rod pull out problem, theory and experiment, J. Mech. Phys. Solids 30, 97-120.

[2] Xanthis, L.S., Bernal, M.J.M. and Atkinson, C. (1981). The treatment of singularities in the calculation of stress intensity factors using the boundary integral equation method, Comp. Methods in Appl. Mechs. and Engng., 26, 285-304.

[3] Atkinson, C., Xanthis, L.S. and Bernal, M.J.M. (1981). Boundary integral equation crack tip analysis and applications to elastic media with spatially varying elastic properties, Comp. Methods in Appl. Mechs. and Engng., 29, 35-49.

[4] Wait, R. (1977). Singular isoparametric finite elements, J. Inst. Maths. Applics. 20, 133-141.

[5] Papamichael, N. and Whiteman, J.R. (1972). A numerical conformal transformation method for harmonic mixed boundary value problems. Brunel University, Dept. of Mathematics, Report No. TR/18.

[6] Symm, G.T. (1973). Treatment of singularities in the solution of Laplace's equation by an integral equation method. NPL Report. NAC 31.

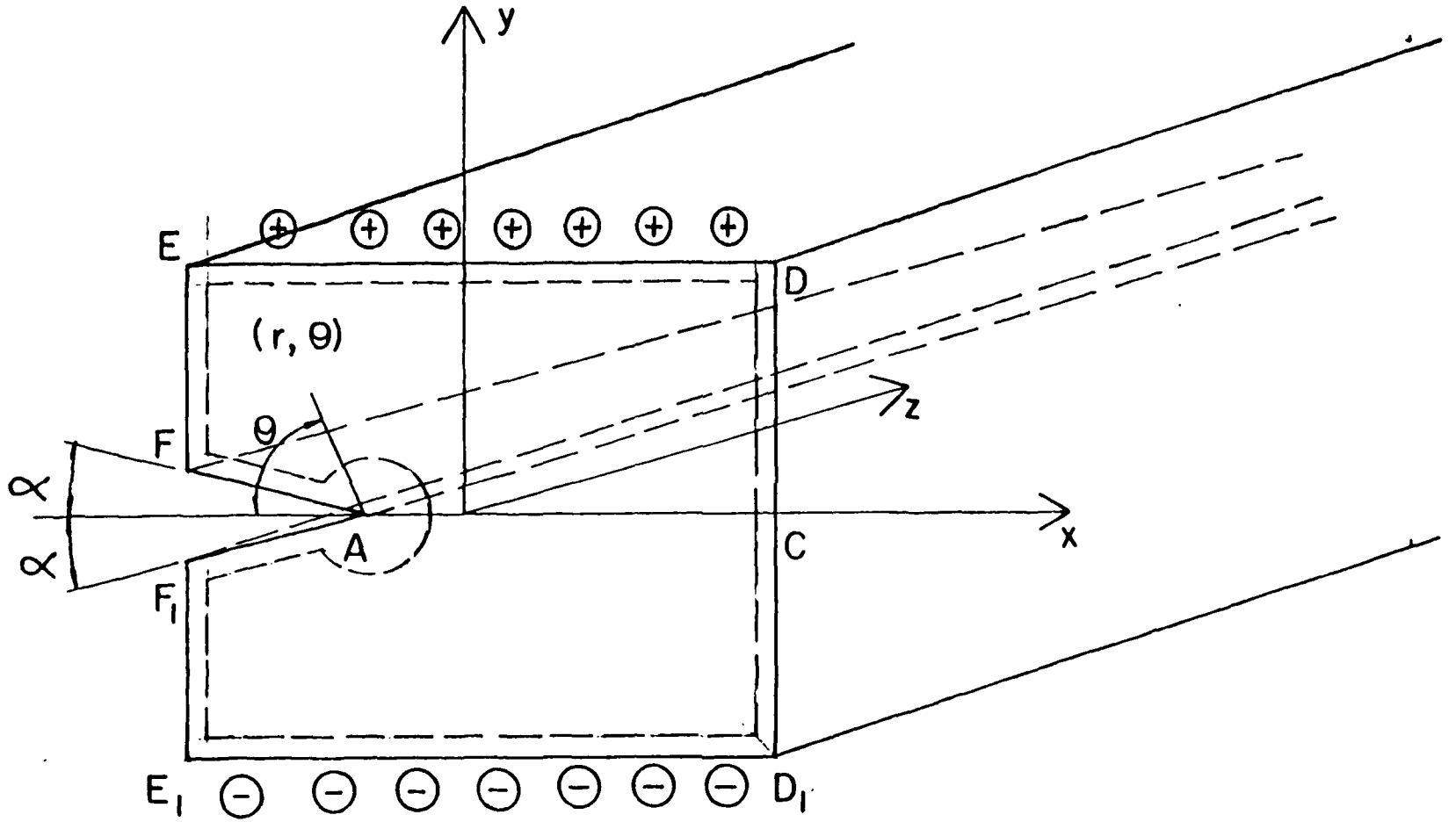

FIGURE .1.

APPENDIX

1. Introduction

In this report the boundary integral equation (B.I.E.) method is discussed with particular reference to its application to fracture mechanics stress analysis. Although the B.I.E. method has been used to treat a variety of boundary value problems, those encountered in fracture mechanics possess certain unique features which require special treatment. There are essentially two distinct difficulties which are encountered when applying standard B.I.E. procedures to fracture models in which a crack is modelled as having a planform of zero thickness (e.g. a line crack in two dimensions).

These are:-

(i) The indeterminacy encountered when (in plane strain or stress), the direct B.I.E. formulation of a thin ellipse is used to represent a crack when the ellipse degenerates to a line. A similar feature occurs in three dimensional problems. We describe this degeneracy more fully later in this introduction, attempts to remove this difficulty are described in section 3.

(ii) The existence of a stress singularity at a sharp crack tip which requires accurate boundary element modelling in order to obtain reliable numerical results. Such modelling is described in detail in section 4. Note however that, although a square root stress singularity occurs in the elastic analysis of a crack in a homogeneous medium, other stress singularities may be encountered (see [1] for a review).

It is worth noting that information about 'stress-intensity factors' (notation to be explained more fully in section 2) can be obtained from stress and displacement fields far from the crack tip by judicious use of certain path independent integrals. Such integrals are discussed in section 2 and their use will be illustrated in section 4.

To understand the first difficulty discussed above we review here the derivation of the direct integral formulation of Rizzo [2]. The boundary integral equations can be deduced via an appropriate reciprocal theorem, fundamental solution and certain limiting processes as field points approach the boundary. For an elastic medium the starting point is Betti's second theorem which states that for continuous, finite stresses and zero body force

$$\int_S t_i u_i^* dS = \int_S t_i^* u_i dS \tag{8.1}$$

where $t_i = \sigma_{ij} n_j$ is the traction vector, u_i is the displacement vector and these together with the field with superscript * denote equilibrium stress states which are well defined at all points in a region R with bounding surface S. In the above reciprocal theorem the stress state with superscript * will be chosen to correspond with the fundamental solution to Navier's equations which for isotropic elasticity can be written:-

Fundamental solutions for two dimensional plane strain (μ is the shear modulus, ν Poisson's ratio)

$$u_i^*(p,q) = [(3-4\nu)\log(1/r)\delta_{ij} + r_{,i}r_{,j}]e_j/8\pi\mu(1-\nu) \tag{8.2}$$

and

$$t_i^*(p,q) = -\frac{1}{r}\{\frac{dr}{dn}[(1-2\nu)\delta_{ij} + 2r_{,i}r_{,j}] - (1-2\nu)[n_j r_{,i} - n_i r_{,j}]\}e_j/4\pi(1-\nu) \tag{8.3}$$

where $r(p,q)$ is the distance between points $p(\underset{\sim}{x})$ with co-ordinates x_i and of $q(\underset{\sim}{x})$ with co-ordinates y_i, then $r_{,i}$ is defined by

$$r_{,i} = \frac{\partial r}{\partial y_i} = -\frac{\partial r}{\partial x_i} \tag{8.4}$$

the e_j are unit vectors. The tractions on an arbitrary surface surrounding the point $p(\underset{\sim}{x})$ can be computed from $u_i^*(p,q)$ by differentiation of $p(\underset{\sim}{x})$ and are given in equation (8.3) above where the normal is taken at $q(\underset{\sim}{x})$. Apart from being a solution of the equilibrium equation when $p \neq q$ the above solution has the significant property that on a small disc S_ε of radius ε centred at the point $p(\underset{\sim}{x})$

$$\lim_{\varepsilon \to 0} \int t_i^* dS = \delta_{ij} e_j \quad . \tag{8.5}$$

Similarly in three dimensions we have:

Fundamental solution in 3 dimensions

$$u_i^*(p,q) = \frac{1}{r(p,q)} [(3-4\nu)\delta_{ij} + r_{,i} r_{,j}] e_j / 16\pi\mu(1-\nu) \tag{8.6}$$

and

$$t_i^*(p,q) = -\frac{1}{r^2} \{\frac{dr}{dn}[(1-2\nu)\delta_{ij} + 3r_{,i} r_{,j}] - (1-2\nu)(n_j r_{,i} - n_i r_{,j})\} e_j / 8\pi(1-\nu) \tag{8.7}$$

where e_j are unit vectors in the co-ordinate directions.

A significant property of this solution is that on a small sphere S_ε of radius ε about the point $p(\underset{\sim}{x})$

$$\lim_{\varepsilon \to 0} \int_{S_\varepsilon} t_i^* \, dS = \delta_{ij} e_j \tag{8.8}$$

Thus the fundamental solution corresponds to the well-known Kelvin problem of a point load in an infinite body. Using the above one can write

$$u_i^*(p,q) = U_{ji}(p,q) e_j ; \quad t_i^*(p,q) = T_{ji}(p,q) e_j \tag{8.9}$$

such that the first index in $U_{ji}(p,q)$ and $T_{ji}(p,q)$ corresponds to the direction of the point load and the second index refers to the component of the respective displacements and tractions.

Since the above fundamental solutions are singular at $p(\underset{\sim}{x})$ we apply equation (8.1) to the region R with a region R_ε (a ball of radius ε around $p(\underset{\sim}{x})$) deleted from it. If this ball has surface S_ε equation (8.1) is rewritten

$$\int_{S+S_\varepsilon} t_i u_i^* dS = \int_{S+S_\varepsilon} u_i t_i^* dS \tag{8.10}$$

The expressions (8.3) and (8.4) or (8.6) and (8.7) for u_i^* and t_i^* are now substituted into equation (8.10) and the stress field $\sigma_{ij}(p)$ and displacement $u_i(p)$ assumed continuous and bounded for any point $p(\underset{\sim}{x})$ belonging to R. The following limiting results are also deduced:-

$$\lim_{\varepsilon \to 0} \int_{S_\varepsilon} t_i u_i^* dS = 0 \tag{8.11}$$

and

$$\lim_{\varepsilon \to 0} \int_{S_\varepsilon} u_i t_i^* dS = u_i(p)\delta_{ij}e_j = u_j(p)e_j \tag{8.12}$$

Using these expressions in equation (8.10) and taking the limit $\varepsilon \to 0$ leads to a standard result at an interior point p

$$u_j(p) = \int_S t_i(Q)U_{ji}(p,Q)dS(Q) - \int_S u_i(Q)T_{ji}(p,Q)dS(Q) \tag{8.13}$$

where the tensors U_{ji} and T_{ji} can be deduced from the definitions (8.9). The above equation thus gives a representation for the displacements at any interior point $p(\underset{\sim}{x})$ and the stresses may be calculated by differentiation with respect to the field point $p(\underset{\sim}{x})$ with co-ordinates x_i. The result can be written

$$\sigma_{ij}(p) = \int_S t_k(Q)D_{kij}(p,Q)dS(Q) - \int_S u_k(Q)S_{kij}(p,Q)dS(Q) \tag{8.14}$$

where the tensors D_{kij} and S_{kij} are determined from U_{ji} and T_{ji} respectively, by differentiation with respect to the field point $p(\underset{\sim}{x})$ and using the stress-strain relations.

The above results give the stress and displacement at an interior point. The well known boundary integral equation is obtained by taking the limiting form of equation (8.13) (sometimes known as Somigliana's identity for the displacement vector) and letting the interior point $p(\underset{\sim}{x})$ tend to a boundary point $P(\underset{\sim}{x})$. Taking due account of the discontinuity of the second integral on the right hand side of equation (8.13) as $p(\underset{\sim}{x}) \to P(\underset{\sim}{x})$ from the interior leads to the integral equation

$$u_j(P)/2 + \int_S u_i(Q)T_{ji}(P,Q)dS(Q) = \int_S t_i(Q)U_{ji}(P,Q)dS(Q) \qquad (8.15)$$

The difficulty with the application of the standard B.I.E. formulation to fracture mechanics has been outlined clearly by Cruse [3,4,5], we follow his derivation here. He considers the two dimensional situation shown in figure 1 where S, Γ^+ and Γ^- represent the regular, upper and lower crack surfaces as shown. The Somigliana identity (equation (8.13)) for the displacement at an interior point $p(\underset{\sim}{x})$ is thus given by

$$u_j(p) = \int_{S+\Gamma^++\Gamma^-} U_{ji}(p,Q)t_i(Q)dS(Q) - \int_{S+\Gamma^++\Gamma^-} T_{ji}(p,Q)u_i(Q)dS(Q) \qquad (8.16)$$

The kernels U_{ji} and T_{ji} are defined in equation (8.9) and have the property that

$$T_{ij}(p,Q^+) = -T_{ij}(p,Q^-) \qquad (8.17)$$

and

$$U_{ij}(p,Q^+) = +U_{ij}(p,Q^-) \qquad (8.18)$$

for Q^+ and Q^- lying on the crack faces Γ^+ and Γ^- respectively except near the small crack tip region. Note that the sign change in (8.17), is due to the opposite normal directions of the two crack surfaces. Letting the

two crack surfaces collapse to the plane Γ (with the same normal as Γ^+) leads to the equation

$$u_j(p) = \int_S U_{ji}(p,Q)t_i(Q)dS(Q) - \int_S T_{ji}(p,Q)u_i(Q)dS(Q)$$
$$- \int_\Gamma T_{ji}(p,Q)\Delta u_i(Q)dS(Q) + \int_\Gamma U_{ji}(p,Q) \quad \Sigma t_i(Q)dS(Q) \tag{8.19}$$

where

$$\Delta u_j(Q) = u_j(Q^+) - u_j(Q^-) \tag{8.20}$$

$$\Sigma t_j(Q) = t_j(Q^+) + t_j(Q^-) \tag{8.21}$$

In general situations are encountered where the crack is loaded by equal and opposite tractions such that $\Sigma t_j(Q) = 0$. The usual next step is to let $p(\underset{\sim}{x}) \to P(\underset{\sim}{x})$ a boundary point in equation (8.19) in order to obtain the boundary integral equation. However, when $P(\underset{\sim}{x})$ is a point on the plane Γ (not at the edge of Γ) the equation becomes

$$u_j(P) - \Delta u_j(P)/2 + \int_S T_{ji}(P,Q)u_i(Q)dS(Q)$$
$$+ \int_\Gamma T_{ji}(P,Q)\Delta u_i(Q)dS(Q) = \int_S U_{ji}(P,Q)t_i(Q)dS(Q) \tag{8.22}$$

where the usual term for the jump in the boundary integral has been taken and the integral over Γ is a principal value integral. Equation (8.22) is deficient in two critical respects. In the first place while a single surface Γ is being treated, two variables are unknown. These are Δu_j and $\Sigma u_j = u_j(P) - \Delta u_j(P)/2$. The second deficiency is that equation (8.22) is the same for any set of equal and opposite crack boundary tractions (i.e. such that $\Sigma t_j(Q) = 0$ where Q lies on Γ). Thus this integral equation cannot deal with situations where the crack is loaded internally.

As a consequence of the above mentioned deficiencies inherent in a straightforward application of the boundary integral equation (8.22) to flat crack modelling, a variety of methods have been suggested which each

deal with special cases. No all purpose method applicable to a variety of unsymmetric crack plan forms seems to be available at the present time. However, a possibility is suggested in section 3, but a practical test of its applicability is yet to be made. A discussion of the variety of methods which have been suggested for special situations will also be made in Section 3. Note, however, that the above-mentioned difficulties are all specific to the sharp crack model of fracture mechanics. Useful numerical results might still be obtained by modelling the crack as an elliptical hole to give an accurate stress field far from the crack and then use invariant integrals to calculate the (sharp) near crack tip stress field. A discussion of such invariant integrals is made in sections 2.2 and 2.3.

2. Stress intensity factors and invariant integrals

As discussed in the introduction there are certain features of the stress anslysis of theoretical fracture models that distinguish these problems from others to which B.I.E. methods have been applied. For completeness we include here a brief description of some of the most commonly used notations and results, notably those pertaining to a crack in a homogeneous elastic body. For situations where cracks meet interfaces between different elastic media or lie along a bimaterial interface different singularities are encountered, for a review of some of these situations see [1].

2.1 Fracture modes and stress intensity factors

A key feature in the stress analysis of the crack models considered here is the singular stress field at the crack tip. For a crack in a homogeneous medium an eigenvalue analysis (see for example Williams [6]) gives a result of the form

$$\sigma \sim KF(\theta)r^{-1/2} + \text{non-singular terms} \qquad (8.23)$$

where (r,θ) are polar-co-ordinates based at the crack tip (see Fig. 2), $F(\theta)$ is a function determined by the eigenvalue analysis and is independent of the applied load or body shape. Thus, close to the crack tip the interaction with the applied stress field is fully characterised by the coefficient K. This coefficient, which depends on the applied load, the shape of the body, and the crack length, is called the stress intensity factor and is a cornerstone of contemporary fracture mechanics. In general, when the applied stress induces stresses on the crack which are a combination of pure tension and shear, there are three stress intensity factors associated with the different modes of fracture. These are illustrated in

Figs 3. A standard notation is to use K_I for the opening (mode I), K_{II} for in-plane sliding (mode II), K_{III} for anti-plane sliding (mode III) modes of relative displacement of the crack surfaces. The following results are standard for isotropic bodies in plane strain, plane stress or anti-plane strain. For the pure opening mode, we have

$$\begin{Bmatrix} \sigma_{11} \\ \sigma_{12} \\ \sigma_{22} \end{Bmatrix} = \frac{K_I}{(2\pi r)^{1/2}} \cos(\theta/2) \begin{Bmatrix} 1 - \sin(\theta/2)\sin(3\theta/2) \\ \sin(\theta/2)\cos(3\theta/2) \\ 1 + \sin(\theta/2)\sin(3\theta/2) \end{Bmatrix} \tag{8.24}$$

for the singular near crack tip stress field, and

$$\begin{Bmatrix} u_1 \\ u_2 \end{Bmatrix} = \frac{K_I}{2\mu} \left(\frac{r}{2\pi}\right)^{\frac{1}{2}} \begin{Bmatrix} \cos(\theta/2)[\kappa-1+2\sin^2(\theta/2)] \\ \sin(\theta/2)[\kappa+1-2\cos^2(\theta/2)] \end{Bmatrix} \tag{8.25}$$

where $\kappa = 3-4\nu$ (plane strain) $\kappa = (3-\nu)/(1+\nu)$ (plane stress).

Note $\sigma_{33} = \nu(\sigma_{11}+\sigma_{22})$ for plane strain. For the in plane sliding mode

$$\begin{Bmatrix} \sigma_{11} \\ \sigma_{12} \\ \sigma_{22} \end{Bmatrix} = \frac{K_{II}}{(2\pi r)^{1/2}} \begin{Bmatrix} -\sin(\theta/2)[2 + \cos(\theta/2)\cos(3\theta/2)] \\ \cos(\theta/2)[1 - \sin(\theta/2)\sin(3\theta/2)] \\ \sin(\theta/2)\cos(\theta/2)\cos(3\theta/2) \end{Bmatrix} \tag{8.26}$$

and

$$\begin{Bmatrix} u_1 \\ u_2 \end{Bmatrix} = \frac{K_{II}}{2\mu} \left(\frac{r}{2\pi}\right)^{\frac{1}{2}} \begin{Bmatrix} \sin(\theta/2)[\kappa + 1 + 2\cos^2(\theta/2)] \\ -\cos(\theta/2)[\kappa - 1 - 2\sin^2(\theta/2)] \end{Bmatrix} \tag{8.27}$$

For anti-plane sliding we have

$$\begin{Bmatrix} \sigma_{13} \\ \sigma_{23} \end{Bmatrix} = \frac{K_{III}}{(2\pi r)^{1/2}} \begin{Bmatrix} -\sin(\theta/2) \\ \cos(\theta/2) \end{Bmatrix} \tag{8.28}$$

and

$$u_3 = 2 \frac{K_{III}}{\mu} \left(\frac{r}{2\pi}\right)^{1/2} \sin(\theta/2) \qquad (8.29)$$

In each of the above ν is Poisson's ratio, μ is the shear modulus, (r,θ) are polar co-ordinates based at the crack tip as shown in Fig. 2, and the crack lies on the plane $x_2 = 0$ as shown in Fig. 2.

It is obvious from the above formulae that the stress intensity factor K is an important parameter characterising the singular near crack tip stress field. It connects with fracture theory through the postulate that fracture will commence (i.e. a crack will grow) when the stress intensity factor reaches a critical value K_c, this value being an experimentally determined material property assumed independent of the shape of the body. Such a fracture criterion is however unambiguous only when a single mode is operative. In a mixed mode situation which occurs for example when a crack is aligned at an angle to an applied tensile stress there is still discussion as to what is the correct fracture criterion to use. We concern ourselves in this article with accurate procedures for calculating the near crack tip stress field for either single or mixed mode situations. The question as to what fracture criterion is best suited to predicting mixed mode fracture will not be addressed, however, see [1] for a review and discussion of this point.

In addition to the above "critical stress intensity factor" fracture criterion there is the 'energy release rate' fracture theory of Griffith. This states that for a pre-existing crack to grow, the decrease of the total energy (elastic energy plus potential energy of the loading mechanism) must be equal to or exceed the surface energy of the two newly created fracture surfaces. The energy release rate, or crack extension force, G, can thus be defined as the amount of energy released from the system

(cracked specimen plus loading mechanism) for unit advance of the crack front. For fracture in either of the three modes shown in Fig 3 , it can be shown that

$$G_I = \frac{K_I^2(1-\nu^2)}{E}, \quad G_{II} = \frac{K_{II}^2(1-\nu^2)}{E}, \quad G_{III} = \frac{K_{III}^2}{\mu} \qquad (8.30)$$

where E is Young's modulus. The Griffith fracture criterion then says that fracture occurs when $G = 2\gamma$ (γ being the surface energy of each of the newly created surfaces). Thus when a single mode is operative the criteria of critical stress intensity factor and critical energy release rate are equivalent. However, in the mixed mode situation for a crack growing in its own plane the energy release rate is

$$G = (K_I^2 + K_{II}^2)\frac{(1-\nu^2)}{E} + \frac{K_{III}^2}{2\mu} \qquad (8.31)$$

and no simple association between the two criteria is possible (cf. reference [1]).

The above discussion applies strictly to elastic media and brittle solids but nevertheless has had quite widespread practical success.

The subject of elastic-plastic fracture mechanics is a modification of the theory described above designed to take into account plastic deformation at a crack tip. A detailed description of this subject is outside the scope of the present article, however the following features are noted (see [1] or [7] for a more complete account.) For problems of small scale yielding the singular solutions outlined in equations (8.24) to (8.29) are useful in setting an 'outer' approximation to the stress field. In models where plastic flow occurs by slip bands emanating from a crack tip such as envisaged by Bilby and Swinden [8] or by superdislocation modelling of plasticity, Atkinson and Kay [9] (see also [10]), it is important to have some information of higher order terms in (8.23) in order

to determine the shear stress induced on the slip band. As we shall see later this information is readily available with certain kinds of element modelling in the B.I.E. integral equation.

Another concept much used in elastic-plastic fracture mechanics is the J-integral introduced by Rice (11). This integral is identical to a certain integral of the energy-momentum tensor discussed by Eshelby (12), in the context of generalised forces on point defects and inhomogeneities in elastic fields. Under certain circumstances integrals based on the energy momentum tensor are invariant and by suitably deforming the contour of the integral, information about near crack tip stress fields can be deduced from numerical information obtained on the boundary of a region removed from the crack tip. A brief derivation of some of these integrals will be given in the next section as a precursor to their numerical implementation in section 4.

2.2 Invariant integrals based on the energy momentum tensor

We have already indicated briefly in section 2.1 how certain invariant integrals can be used as tools for deducing numerical values of stress intensity factors. Here a simple deduction of integrals which can be derived from a (perhaps pseudo) energy momentum tensor is made. The prescription used is similar to that described by Eshelby [13] although equivalent results can be obtained by a formal application of Noether's theorem (see Knowles and Sternberg [14] and for somewhat equivalent earlier work by Gunther [15]).

We suppose a Lagrangian (L) is given which has the property that the conditions of stationarity of the functional $\int L \, dv$ (where v is the volume of the body) lead to Euler equations which are themselves the field equations of the continuum being studied. In order to retain some generality suppose

$$L = L(X_i, u_i, u_{i,j}, \phi_i, \uparrow_{i,j}) \tag{8.32}$$

thus L depends on position (cartesian co-ordinates X_i) and two independent vector fields u_i, ϕ_i and their gradients $u_{i,j} = \partial u_i/\partial X_j$ etc. . The Euler equations are thus

$$\frac{\partial}{\partial X_j}\left(\frac{\partial L}{\partial u_{i,j}}\right) - \frac{\partial L}{\partial u_i} = 0 \quad \text{and} \quad \frac{\partial}{\partial X_j}\left(\frac{\partial L}{\partial \phi_{i,j}}\right) - \frac{\partial L}{\partial \phi_i} = 0 \tag{8.33}$$

and the summation convention with respect to repeated indices ($i = 1,2,3$) has been used. If we now define the tensor

$$P_{j\ell} = \frac{\partial L}{\partial u_{i,j}} u_{i,\ell} + \frac{\partial L}{\partial \phi_{i,j}} \phi_{i,\ell} - L\delta_{j\ell} \tag{8.34}$$

then it can be shown by direct calculation, using the above Euler equations, that

$$\frac{\partial P_{j\ell}}{\partial X_j} = -\left(\frac{\partial L}{\partial X_\ell}\right)_{exp} \tag{8.35}$$

where $(\partial L/\partial X_\ell)_{exp}$ means that all variables are held constant except explicit dependence on X_ℓ. This last equation is important because it means that if we define the integrals

$$F_\ell = \int_S P_{j\ell}\, dS_j \tag{8.36}$$

where S is a specified surface, then if the surface integral encloses a volume in which there are no singularities, use of the divergence theorem and equation (8.35) reduce the corresponding volume integral to zero provided L does notdepend explicitly on X_ℓ. This means that a surface integral taken around a crack tip can be related to an integral far from the tip and since under favourable circumstances the near tip integral can be calculated directly in terms of a single unknown stress intensity factor, this gives an independent method of stress intensity

factor evaluation. It should be stressed however that this is only possible provided the appropriate components of $P_{j\ell}$ are zero along the crack surface. When this last condition is satisfied the near tip integral will be exactly equal to the integral evaluated far from the crack tip if L does not depend explicitly on the spatial co-ordinate X_ℓ.

We illustrate the above procedure with two fairly general examples (the standard example of classical elasticity will be included as a special case). The first example we consider is that of micropolar elasticity (cf Atkinson [16] for a more complete account).

2.2.1 Application to Micropolar Elasticity.

The theory of micropolar elasticity is reviewed by Eringen [17] and depends on the usual elastic strain tensor together with an independent 'microrotation vector'. For a discussion of the limitations of the classical couple-stress theory and its relation to the micropolar theory the reader is referred to [17].

We suppose there exists a strain energy density function

$$W = W(u_{i,k},\ \phi_j, \phi_{j,s}) \tag{8.37}$$

where ϕ_j is the micro-rotation vector and a comma denotes partial differentiation with respect to the cartesian co-ordinates (X_1, X_2, X_3). We assume that W has the property that

$$t_{\ell k} = \frac{\partial W}{\partial u_{k,\ell}}\ , \quad m_{\ell k} = \frac{\partial W}{\partial \phi_{k,\ell}} \quad \text{and} \quad \frac{\partial W}{\partial \phi_N} = \varepsilon_{\ell kN} t_{k\ell} \tag{8.38}$$

Replacing L by -W in equations (8.33) above leads to the Euler equation for minimising the functional $\int W\, dV$. In terms of the stresses $(t_{\ell k})$ and couple stresses $(m_{\ell k})$ defined above, these equilibrium equations can be written

$$\frac{\partial t_{j\ell}}{\partial X_j} = 0 \; ; \qquad \frac{\partial m_{j\ell}}{\partial X_j} - \epsilon_{\ell ki} t_{kj} = 0 \tag{8.39}$$

The energy momentum tensor defined in equation (8.34) is thus

$$P_{j\ell} = W\delta_{j\ell} - t_{ji} u_{i,\ell} - m_{ji} \phi_{i,\ell} \tag{8.40}$$

where we note that the first index denotes the normal direction, i.e. $t_{j\ell}$ is the stress in direction ℓ acting on a plane of normal j. The rest of the theory discussed above also applies to this case. For example for a plane crack the crack extension force or energy release rate (G) can be defined as

$$G = F_1 = \int_S P_{j1} dS_j \tag{8.41}$$

where S is a surface enclosing the crack tip (in the 2d case this is a cylinder with generators parallel to the X_3 axis so that the integral in (8.41) is effectively a line integral in the (X_1, X_2) plane). Note, also that for a stress free crack the tractions t_{2i} and the couple stresses m_{2i} will be zero so the integrand P_{21} is zero on the crack faces and the integral defining G taken around the crack tip for an edge crack can be deformed into the far field provided only that the energy-density W does not depend explicitly on X_1 (compare equation (8.35)).

Thus for micropolar elasticity the invariant integral F_1 can be used to determine the energy release from numerical information derived at points remote from the crack tip. It should be noted however that it is not possible in general to extract the crack tip stress intensity factor from this information since the energy release rate contains a couple stress intensity factor contribution in addition to the classical elastic contribution. For more information on this point and a detailed analysis of the internal crack problem in micropolar elastic media see Atkinson and Leppington [18].

The above analysis applies also, of course, to classical elasticity when ϕ_i is identically zero, the stress tensor $t_{k\ell}$ then being symmetric in the linear theory.

2.2.2. Coupled, time dependent, linear thermoelasticity and thermoviscoelasticity

Recently Atkinson and Smelser [19] have applied a procedure similar to that outlined above to the equations of coupled time dependent thermoviscoelasticity under conditions applicable to stationary cracks disturbing time dependent temperature and stress fields. Initial conditions are considered in which

$$\theta(t) = u_i(t) = \sigma_{ij}(t) = 0 \qquad \text{for } t < 0 \tag{8.42}$$

u_i and σ_{ij} are the usual displacement vector and stress tensor, $\theta(t)$ denotes the infinitesimal temperature deviation from the base temperature T_0. The formulation described in [19] begins by Laplace-transforming the equations of motion etc. which become

$$\begin{aligned} &\bar{\sigma}_{ij,j} = \rho p^2 \bar{u}_i \\ &\bar{\epsilon}_{ij} = \frac{1}{2}(u_{i,j} + u_{j,i}) \\ &\bar{\sigma}_{ij} = p\,\bar{G}_{ijk\ell}\,\bar{\epsilon}_{k\ell} - p\,\bar{\phi}_{ij}\,\bar{\theta} \qquad \text{(anisotropic)} \end{aligned} \tag{8.43}$$

and for the temperature

$$(k_{ij}/T_0)\bar{\theta}_{,ij} = p^2 \bar{m}\,\bar{\theta} + p^2 \bar{\phi}_{ij}\,\bar{\epsilon}_{ij} \tag{8.44}$$

where the Laplace transform is defined by

$$\bar{f}(p) = \int_0^\infty e^{-pt} f(t)dt \,. \tag{8.45}$$

In general for viscoelastic media the coefficients $\bar{G}_{ijk\ell}$ etc. will be functions of p the transform variable.

The above field equations can be generated from a Lagrangian defined as

$$L = -\frac{1}{2}\bar{t}_{ij}\bar{\epsilon}_{ij} - \frac{\rho p^2}{2}\bar{u}_i\bar{u}_i + p\bar{\$}_{ij}\bar{\theta}\bar{u}_{i,j}$$

$$+ \frac{1}{2T_0 p}k_{ij}\bar{\theta}_{,i}\bar{\theta}_{,j} + \frac{1}{2}p\bar{m}\bar{\theta}^2 \qquad (8.46)$$

where $$\bar{t}_{ij} = p\bar{G}_{ijk\ell}\bar{\epsilon}_{k\ell} \qquad (8.47)$$

A 'pseudo' energy momentum tensor is then defined as

$$P_{\ell j} = \frac{\partial L}{\partial \bar{u}_{i,j}}\bar{u}_{i,\ell} + \frac{\partial L}{\partial \bar{\theta}_{,j}}\bar{\theta}_{,\ell} - L\delta_{\ell j} \qquad (8.48)$$

so that we deduce that

$$P_{\ell j} = -(\bar{t}_{ij} - p\bar{\theta}\bar{\phi}_{ij})\bar{u}_{i,\ell} + \frac{k_{ij}}{T_0 p}\bar{\theta}_{,i}\bar{\theta}_{,\ell} - L\delta_{\ell j} \qquad (8.49)$$

and the integrals

$$F_\ell = \int_S P_{\ell j}\, dS_j \qquad (8.50)$$

follow as described earlier. A useful property of the integral F_1 in this case is that provided either the temperature θ is constant or the flux $k_{i2}\bar{\theta}_{,i}$ is zero on the crack faces then P_{12} is zero on the crack face for a stress free crack. Thus in this case the integral can be deformed into the far field as discussed earlier. Also the near field integral, a small contour round the crack tip can be explicitly evaluated in terms of the coefficients of singular transformed stresses $\bar{\sigma}_{ij}$ and temperature gradients $\bar{\theta}_{,i}$. In favourable circumstances explicit determination of these coefficients can be made, see [19] for some applications of these results.

2.2.3 L and M integrals in elastostatics

In the above we have discussed the integrals F_ℓ associated with the tensor $P_{\ell j}$ paying particular attention to the integral F_1 which can be shown to be related to the energy release rate G. Under certain conditions other invariant integrals can be derived from $P_{\ell j}$ and are sometimes useful. We describe these briefly. In addition to the F_ℓ integrals obtained in section 2.2, Gunther [15] obtained for elastostatics the path-independent integrals

$$L_i = \varepsilon_{ik\ell} \int_S (x_k P_{\ell j} + u_k P_{\ell j})\, dS_j \tag{8.51}$$

and

$$M = \int_S (x_\ell P_{\ell j} - \frac{1}{2} u_\ell P_{\ell j})\, dS_j \tag{8.52}$$

where ℓ, j, k take the values 1, 2 and 3 and $P_{\ell j} = \partial W(u_{m,n})/\partial u_{\ell,j}$ is the Boussinesq or first Piola-Kirchoff stress-tensor which gives the component parallel to the (rectangular) X_i co-ordinate axis of the force on a surface element which was of unit area and perpendicular to the X_j axis before deformation. The energy momentum tensor is defined as in equation (8.34) with $L = -W$ and the energy density W is a function of $u_{m,n} = \partial u_m/\partial X_n$ with $n = 1$, 2 or 3, ε_{ijk} is the permutation tensor.

In section (2.2) it is shown that the integrals F_ℓ will be path independent if $L = -W$ does not depend explicitly on X_ℓ. The deformation may be non-linear and the material may be non-linear but the energy density must be homogeneous if each of the F_ℓ is to be path independent. For the integrals L_i these conditions are the same and in addition the material must be isotropic.

In a two dimensional state of plane strain (8.52) reduces to

$$M = \int_S x_\ell\, P_{\ell j}\, dS_j \tag{8.53}$$

taken along a plane curve S with normal (n_1, n_2). Summation over i and j is now only over 1 and 2. An application of the F_ℓ and M integrals to the case of anti-plane strain is made in section 4 to obtain crack tip stress intensity factors from numerical information far from the crack tip.

2.3 Invariant integrals deduced from Betti's reciprocal theorem

The integrals discussed in section 2.2 have the disadvantage that they give energy release rates or related quantities but explicit determination of stress intensity factors may not be possible when mixed mode situations are encountered. It should be noted however that the general approach of section (2.2) (equations (8.33) to (8.36)) is not restricted to linear stress-strain laws. An alternative approach has been developed by Stern and co-workers [20] to [24] who derive invariant integrals for plane linear elastic problems by means of Betti's reciprocal theorem.

The starting point of their analysis is the reciprocal theorem written as

$$\int_{\partial R^*} (\underline{T}.\hat{\underline{u}} - \hat{\underline{T}}.\underline{u})\, ds = 0 \qquad (8.54)$$

where ∂R^* is the boundary of a plane simply connected bounded region R^*. The states (σ_{ij}, u_i) and $(\hat{\sigma}_{ij}, \hat{u}_i)$ are two distinct equilibrium states (σ_{ij}, u_i) being the state corresponding to a given boundary value problem the other state is an auxiliary one; $\underline{T}$ and $\hat{\underline{T}}$ are the boundary tractions associated with these elastic states. For plane crack problems a contour ∂R^* such as that shown in Fig. 4 is taken.

The idea of the method is to choose the auxiliary state so that the integral around C_ε gives the coefficient of the required stress-singularity as ε tends to zero. For a crack problem if the auxiliary solution also satisfies the stress free boundary condition along the crack it is possible to relate the integral around C_ε to the integral around C_0 by using equation (8.54). The result is that

$$\lim_{\varepsilon \to 0} \int_{C_\varepsilon} (\underline{T}.\hat{\underline{u}} - \hat{\underline{T}}.\underline{u})ds = \int_{C_0} (\underline{T}.\hat{\underline{u}} - \hat{\underline{T}}.\underline{u})\, ds \qquad (8.55)$$

Now the stresses and displacements in the neighbourhood of the crack tip referred to the natural polar co-ordinate system shown in Fig. 4 are:-

$$u_r - u_r^0 = \frac{1}{4\mu}\left(\frac{r}{2\pi}\right)^{1/2}\left\{\left[(2\kappa-1)\cos\frac{\theta}{2} - \cos\frac{3\theta}{2}\right]K_I - \left[(2\kappa-1)\sin\frac{\theta}{2} - 3\sin\frac{3\theta}{2}\right]K_{II}\right\} + o(r^{1/2})$$

$$u_\theta - u_\theta^0 = \frac{1}{4\mu}\left(\frac{r}{2\pi}\right)^{\frac{1}{2}}\left\{\left[-(2\kappa+1)\sin\frac{\theta}{2} + \sin\frac{3\theta}{2}\right]K_I - \left[(2\kappa+1)\cos\frac{\theta}{2} - 3\cos\frac{3\theta}{2}\right]K_{II}\right\} + o(r^{\frac{1}{2}})$$

$$\sigma_r = \frac{1}{4(2\pi r)^{\frac{1}{2}}}\left\{\left(5\cos\frac{\theta}{2} - \cos\frac{3\theta}{2}\right)K_I - \left(5\sin\frac{\theta}{2} - 3\sin\frac{3\theta}{2}\right)K_{II}\right\} + o(r^{-\frac{1}{2}}) \qquad (8.56)$$

$$\sigma_\theta = \frac{1}{4(2\pi r)^{\frac{1}{2}}}\left\{\left(3\cos\frac{\theta}{2} + \cos\frac{3\theta}{2}\right)K_I - \left(3\sin\frac{\theta}{2} + 3\sin\frac{3\theta}{2}\right)K_{II}\right\} + o(r^{-\frac{1}{2}})$$

$$\sigma_{r\theta} = \frac{1}{4(2\pi r)^{\frac{1}{2}}}\left\{\left(\sin\frac{\theta}{2} + \sin\frac{3\theta}{2}\right)K_I + \left(\cos\frac{\theta}{2} + 3\cos\frac{3\theta}{2}\right)K_{II}\right\} + o(r^{-\frac{1}{2}})$$

where u_r^0 and u_θ^0 are the radial and tangential components of the displacement $\underline{u}^0$ of the crack tip and

$$K_I = \lim_{r\to 0} (2\pi r)^{\frac{1}{2}}\sigma_\theta\big|_{\theta=0}$$
$$K_{II} = \lim_{r\to 0} (2\pi r)^{\frac{1}{2}}\sigma_{r\theta}\big|_{\theta=0} \qquad (8.57)$$

are the conventional stress intensity factors. The remainder terms are of the order indicated in distance from the crack tip.

Thus when C_ε is a small circular contour close to the crack tip, $ds = rd\theta$, and the dominant contribution from the traction $\underline{T}$ involves the stress intensity factors multiplying spatially varying terms proportional

to $r^{-1/2}$. Hence if the auxiliary displacement $\hat{\underline{u}}$ can be chosen to have dominant behavior proportional to $r^{-1/2}$ as r tends to zero the product of $\underline{T}.\hat{\underline{u}}$ with ds will have a non-zero finite limit as ε tends to zero. Similarly the traction $\hat{\underline{T}}$ which will now be proportional to $r^{-3/2}$ as r tends to zero will lead to the required 1/r behavior in the product $\hat{\underline{T}}.(\underline{u}-\underline{u}^{0})$. The only stipulation is that $\hat{\underline{u}}$ and $\hat{\underline{T}}$ must be equilibrium solutions and moreover must satisfy the stress free crack boundary conditions. For elastic problems an <u>exact</u> solution of the field equations satisfying stress free boundary conditions can be found by an eigenfunction approach. The auxiliary elastic field required for the above problem has been given by Stern et al [20] as:-

$$\hat{u}_r = \frac{1}{2(2\pi r)^{\frac{1}{2}}(1+\kappa)}\{[(2\kappa+1)\cos\frac{3\theta}{2} - 3\cos\frac{\theta}{2}]c_1 + [(2\kappa+1)\sin\frac{3\theta}{2} - \sin\frac{\theta}{2}]c_2\}$$

$$\hat{u}_\theta = \frac{1}{2(2\pi r)^{\frac{1}{2}}(1+\kappa)}\{[-(2\kappa-1)\sin\frac{3\theta}{2} + 3\sin\frac{\theta}{2}]c_1 + [(2\kappa-1)\cos\frac{3\theta}{2} - \cos\frac{\theta}{2}]c_2\}$$

$$\hat{\sigma}_r = -\frac{\mu}{2(2\pi r^3)^{\frac{1}{2}}(1+\kappa)}\{[7\cos\frac{3\theta}{2} - 3\cos\frac{\theta}{2}]c_1 + [7\sin\frac{3\theta}{2} - \sin\frac{\theta}{2}]c_2\}$$

$$\hat{\sigma}_\theta = -\frac{\mu}{2(2\pi r^3)^{\frac{1}{2}}(1+\kappa)}\{[\cos\frac{3\theta}{2} + 3\cos\frac{\theta}{2}]c_1 + [\sin\frac{3\theta}{2} + \sin\frac{\theta}{2}]c_2\} \qquad (8.58)$$

$$\hat{\sigma}_{r\theta} = -\frac{\mu}{2(2\pi r^3)^{\frac{1}{2}}(1+\kappa)}\{3[\sin\frac{3\theta}{2} + \sin\frac{\theta}{2}]c_1 - [\cos\frac{3\theta}{2} + \cos\frac{\theta}{2}]c_2\}$$

where c_1 and c_2 are arbitrary constants.

Now on the inner circular boundary the evaluation of the contour integral in terms of the traction and displacement (relative to that of the crack tip) components takes the form

$$I_\varepsilon = -\int_{C_\varepsilon} [(\underline{u} - \underline{u}^0)\cdot\hat{\underline{t}} - \hat{\underline{u}}\cdot\underline{t}]ds$$

$$= \int_{-\pi}^{\pi} [\hat{\sigma}_r(u_r - u_r^0) - \hat{\sigma}_{r\theta}(u_\theta - u_\theta^0) - \sigma_r\hat{u}_r + \sigma_{r\theta}\hat{u}_\theta]r\, d\theta.$$

Upon substitution from (8.56) and (8.58), a routine evaluation of the integral produces

$$I_\varepsilon = c_1K_I + c_2K_{II} + o(1) \tag{8.59}$$

where the remainder term goes to zero with ε as indicated. Thus, for arbitrarily small ε (8.55) produces the representation formula

$$c_1K_I + c_2K_{II} = \int_C [(\underline{u}-\underline{u}^0)\cdot\hat{\underline{t}} - \hat{\underline{u}}\cdot\underline{t}]ds \tag{8.60}$$

where it is important to note that the contour C involves only the outer boundary since both $\underline{t}$ and $\hat{\underline{t}}$ necessarily vanish on the crack faces. Furthermore, the rigid body displacement $\underline{u}^0$ may be discarded in the evaluation of (8.60) since the contribution of $\underline{u}^0\cdot\hat{\underline{t}}$ on any closed contour vanishes even when the origin is contained in the interior. It remains only to obtain $\underline{u}$ and $\underline{t}$ on the outer boundary from the prescribed data so that the contour integral may be evaluated as a linear combination of c_1 and c_2, the coefficients of which are the desired stress intensity factors K_I and K_{II}.

The idea of the above method can in principle be extended to a number of other situations, however a major restriction is that the auxiliary solution must be a full solution of the equilibrium equations. Nevertheless, for a variety of elastic problems such solutions can be found and Stern and co-workers have applied the method to a number of other problems ([21] to [24]). An obvious advantage of the method is of course the computation of near field crack tip information from an integral evaluated far from the crack tip.

3. Integral equation methods for crack tip stress analysis

A variety of integral equation methods have been suggested in order to overcome the difficulties outlined in the introduction. However, most of these methods have been designed to treat a special class of problems and are not easily generalised. In the following subsections these methods are outlined.

We begin by briefly discussing how the integral equation (8.15) can be used for the fracture problem. In section 3.1 it is shown how symmetry can be used, in certain cases, to reduce the problem to a boundary value problem for which the formulation discussed in the introduction (equation (8.15)) is appropriate. In section 3.2 partitioning, dividing the body into regions, is used together with continuity conditions along an extension of the crack boundary to couple the two regions together. In both these methods integral equations like equation (8.15) are used so no special attention is paid to the crack as far as the integral equation formulation is concerned. In section 4 we discuss various ways of approximating the integral equation in order to accurately model the crack.

In sections 3.3-3.6 we discuss integral equation formulations which pay particular attention to the crack geometry. In section 3.3 a method which uses exact 'source-crack' Green's functions is outlined. The limitation of this method is that, except for special crack configurations (e.g. straight cracks in plane strain or stress), very few of these Green's functions are known. In section 3.4 straight cracks modelled by Volterra dislocations are considered, thus an integral equation is obtained for the crack in terms of a continuous distribution of (virtual) dislocations. This is coupled to a boundary integral formulation such as that of equation (8.15) in order to deal with finite specimens. The limitation of this approach is that only plane problems and straight cracks are envisaged. Nevertheless, it is natural to represent the crack by elements which

represent a jump in displacement and the dislocation is a fundamental unit of this kind. More fundamental than a Volterra dislocation, however, is the Somigliana dislocation which is an infinitesimal dislocation of area dS with an associated discontinuity vector b_j (representing the jump in displacement u_j across dS) which is effectively constant over the small area dS. We discuss crack modelling by Somigliana dislocations in Section 3.5. Finally, in section 3.6 we show how the dislocation models of sections 3.4 and 3.5 can be derived naturally from Betti's reciprocal theorem.

3.1 Use of symmetry (where possible) to replace crack by boundary value problem

Fig 5 here

For certain symmetric geometries and loading conditions it is possible to replace a crack problem by a mixed boundary value problem and thus apply the standard boundary integral equation of equation (8.15). We illustrate this approach by considering a fracture specimen such as shown in Fig. 5. If the applied loading is tensile and symmetric with respect to $x_2 = 0$, it is clear that fracture should occur in the opening mode and the stress analysis of the configuration (Fig. 5) will lead to a mode I stress intensity factor. Using the symmetry of the specimen it is sufficient to analyse the region $x_2 \geq 0$. For a traction free crack the boundary conditions on $x_2 = 0$ can be written

$$\begin{aligned} t_1 &= 0 \qquad \text{on } x_2 = 0 \qquad x_1 \in AD \\ t_2 &= 0 \qquad \text{on } x_2 = 0 \qquad x_1 \in AO \\ u_2 &= 0 \qquad \text{on } x_2 = 0 \qquad x_1 \in OD \ . \end{aligned} \tag{8.61}$$

The usual notation for stress and displacement has been used, e.g. (u_1,u_2) are the displacements in the (x_1,x_2) directions, and the traction $t_i = \sigma_{ij} n_j$, n_j being the components of the outward drawn normal. We write the integral

equation (8.15) in the equivalent form

$$\int_S [u_i(Q) - u_i(P)]T_{ji}(P,Q)dS(Q) = \int_S t_i(Q)U_{ji}(P,Q)dS(Q) \tag{8.62}$$

where S is the boundary ABCD, i = 1,2, and the integral equation is to be satisfied for all P ∈ S. With either the traction vector t_i or displacement vector u_i specified on the boundary ABCD, consistent with the assumed symmetry, the above integral equation can be reduced to a system of simultaneous equations as discussed in section 4 or elsewhere in this series. Of course accurate element modelling is required to obtain good results for the singular crack tip stresses etc. Note that the integral equation is required along the whole of boundary AD whereas the attempt to directly model the crack boundary discussed in the introduction would have led (if successful) to an integral equation only along the crack AO in addition to the external boundary.

For some early work on applications of this method to fracture specimens where a symmetry plane allows the problem to be set up as a boundary value problem see, e.g. Cruse and Van Buren [25]. In [25] the thickness of the fracture specimen was taken into account, the boundary and crack surfaces being divided into triangles in which the displacements and tractions are assumed constant. In section 4 we show, for an anti-plane elastic problem, how more refined element modelling can be effective.

3.2 Partitioning (subdividing the body into distinct regions)

When there is no symmetry in the cracked specimen it is still possible to get a formulation like that obtained in the last section by subdividing the body into regions. We illustrate this approach by considering the configuration shown in Figure 6. For convenience we denote the part of the boundary described by ABCDA as Γ_1 and the part described by ADEFA as Γ_2.

Then applying the integral equation (8.62) to both regions (i) and (ii) gives the equations

$$\int_{\Gamma_1} [u_i^{(1)}(Q) - u_i^{(1)}(P)]T_{ji}(P,Q)dS(Q) = \int_{\Gamma_1} t_i^{(1)}(Q)U_{ji}(P,Q)dS(Q) \tag{8.63}$$

and

$$\int_{\Gamma_2} [u_i^{(2)}(Q) - u_i^{(2)}(P)]T_{ji}(P,Q)dS(Q) = \int_{\Gamma_2} t_i^{(2)}(Q)U_{ji}(P,Q)dS(Q) \tag{8.64}$$

Along the common boundary AD we have the boundary conditions:-

(i) Continuity of stress, i.e. $t_i^{(1)} = -t_i^{(2)}$ for all points on AD.

(ii) Traction free crack condition $t_i = 0$ on AO.

(iii) Continuity of displacement on OD, $u_i^{(1)} = u_i^{(2)}$ on OD.

It is possible to treat the above equations in the usual way although, of course, accurate modelling is required in order to obtain reliable results. For an early application of this approach see, e.g. Rizzo and Shippy [26] where a formulation of this kind is given for non-homogeneous (two dimensional) inclusion problems.

3.3 The use of exact 'source-crack' Green's functions

One way of avoiding the difficulty discussed in the introduction is to avoid the crack altogether by using as a source function in the integral equation formulation the solution to the problem of a point source, placed anywhere, and a crack in an infinite medium. This approach thus relies on the availability of such a solution and requires that the solution be

known at all points of the body, i.e. in particular at the boundary of the body where the integral equation is applied. These requirements restrict the applicability of such an approach since solutions are known only for special crack geometries. In three dimensions, for example, a crack with a flat elliptical planform is about the limit of cases that can be treated by exact analysis and the stress field everywhere takes on a very complicated form. Some applications of this method to problems of plane anisotropic elasticity have been made by Snyder and Cruse [27]. The resulting integral equation on the boundary B takes the form

$$u_j(z_0)/2 + \int_B T'_{ji}(z_k,z_0)u_i(z_k)dS(z_k) = \int_B U'_{ji}(z_k,z_0)t_i(z_k)dS(z_k) \qquad (8.65)$$

where $z_0 = x_{10} + ix_{20}$ is a point on the boundary B, $z_k = x_{1k} + ix_{2k}$, and the integrals are to be interpreted in the principal value sense. The displacements and tractions U'_{ji} and T'_{ji} are derived from the fundamental solution for the infinite plate with a crack lying on $x_2 = 0 \quad -a < x_1 < a$ and with unit loads applied in the x_j direction acting at some point (x_{10},x_{20}) not lying on the crack. The functions U'_{ji} and T'_{ji} given in [27] are for orthotropic materials. Note however the corrections indicated in the later paper by Cruse [5]. Thus in their applications only mode I and II stress intensity factors are found. It should be noted however that for general anisotropic solids, plane elastic problems can result in stress intensity factors of modes I, II and III even though the displacement field does not vary in the three direction. The method of this section can be extended to this situation also, see the papers [28,29,30] for information on the necessary fundamental solutions.

As discussed earlier it is only for certain special problems that the fundamental solution of the unit load-crack interaction is known in a suitably compact form and thus this method is of limited application.

Nevertheless, for completeness we briefly sketch the derivation of equation (8.65) following [27]. Betti's reciprocal theorem in the absence of body forces can be written

$$\int_{B+L+\Gamma} T'_{ji} u_i \, dS = \int_{B+L+\Gamma} U'_{ji} t_i \, dS \tag{8.66}$$

where L is the crack boundary, B the boundary of the body, and Γ is a circle of vanishing radius ε surrounding the unit load applied at the point (x_{10}, x_{20}). Since the crack L is assumed to be traction free the integrals in equation (8.66) over the crack L are both identically zero, i.e.

$$\int_{L} T'_{ji} u_i \, dS = \int_{L} U'_{ji} t_i \, dS = 0 \tag{8.67}$$

The boundary integral equation (8.65) is thus derived in the usual manner by letting $\Gamma \to 0$ and $(x_{10}, x_{20}) \to B$.

In [31] a somewhat similar situation is considered.

3.4 Integral equations for ideal crack geometries

In the last section the crack problem was treated by using, as a fundamental solution, the complete stress and displacement field due to a unit force interacting with a crack. However, as indicated in that section such solutions are known only for a special class of crack geometries e.g. straight cracks in plane strain configurations. The next stage in versatility is perhaps reached by modelling the crack by extended dislocations (Volterra dislocations). Crack problems formulated in this way have been reviewed by Bilby and Eshelby [32] for the homogeneous medium case, and integral equations for cracks in bimaterials have been derived and treated numerically in Atkinson [33] and Cook and Erdogan [34]. This approach has been coupled, with the boundary integral equation method (8.15), by Rudolph and Ashbaugh [35]. They treat the two dimensional problem of a

finite length crack in a bounded linearly elastic isotropic medium subjected to in plane forces. The superposition principle is used to couple together the B.I.E. method applied to the unflawed medium with boundary stresses those induced on the boundary by the 'perturbed problem', that of a crack in an infinite medium. Since this 'perturbed problem' must represent a stress free crack, the traction on the crack surface must be zero thus producing an integral equation along the crack surface which involves the interior stresses induced at the crack boundary by the B.I.E. solution, hence coupling the two problems.

The treatment given in [35] concentrates on a mode I problem (hence a certain amount of symmetry is assumed), although in principle the method can be applied (to straight cracks) when there are other modes present (such a situation is considered by Chang and Morgan [36]). The stress field of a mode I crack in an infinite medium is expressed in terms of a density of virtual edge dislocations $f(\xi)$ in the form

$$u_i^{(2)}(\underset{\sim}{x}) = \frac{1}{\pi(\kappa+1)} \int_{-1}^{1} f(\xi) K_i(\underset{\sim}{x},\xi)\, d\xi$$

$$\frac{1}{\mu}\sigma_{ij}^{(2)}(\underset{\sim}{x}) = \frac{4}{\pi(\kappa+1)} \int_{-1}^{1} f(\xi) K_{ij}(\underset{\sim}{x},\xi)\, d\xi \qquad (8.68)$$

where

$$K_1 = (\kappa-1)\ln r^2 - 4x_2^2/r^2$$

$$K_2 = -2(\kappa+1)\arctan\left(\frac{\xi-x_1}{x_2}\right) - \frac{4x_2(\xi-x_1)}{r^2} \qquad (8.69)$$

$r^2 = (\xi-x_1)^2 + x_2^2$ and the kernels K_{ij} can be derived from the K_i by differentiation. Note that the dislocation density can be expressed in terms of the u_2 displacement by

$$f(x_1) = \frac{\partial}{\partial x_1}\left[u_2^{(2)}(x_1,0^+)\right] = -\frac{\partial}{\partial x_1}\left[u_2^{(2)}(x_1,0^-)\right] \tag{8.70}$$

where the crack is taken to lie on $x_2 = 0$, $-1 < x_1 < 1$.

The solutions for the 'unflawed medium' problem (designed by a superscript (1) in our notation) and the crack in an infinite medium (designated by superscript (2)) are now combined to obtain the solution for the original problem. Let C_i^u denote that portion of C where u_i is specified and C_i^t denote that portion where t_i is specified, then

$$C = C_i^u + C_i^t \qquad i = 1,2$$

and (8.71)

$$u_i^{(1)}(P) + u_i^{(2)}(P) = u_i(P), \qquad P \in C_i^u$$

$$t_i^{(1)}(P) + t_i^{(2)}(P) = t_i(P), \qquad P \in C_i^t$$

where $u_i(P)$ and $t_i(P)$ are the specified boundary displacements and tractions of the original problem.

Also for $|x_1| < 1$, $x_2 = 0$

$$t_2^{(1)}(x_1,0) + t_2^{(2)}(x_1,0) = 0 \tag{8.72}$$

$$t_1^{(1)}(x_1,0) = 0$$

the last condition is an implied restriction on the symmetry of the boundary C and loading system such that only one fracture mode is operative (mode I). [Note of course that

$$t_2(x_1,0) \equiv \sigma_{22}(x_1,0) \quad \text{and} \quad t_1(x_1,0) \equiv \sigma_{12}(x_1,0) \ ]$$

The use of the above conditions leads to a pair of coupled integral equations, the integral over C being of the usual B.I.E. type. The integral equation along the crack has a Cauchy integral part due to the dislocation representation of the crack. Thus from equation (8.68) the normal stress

on the crack line reduces to

$$t_2^{(2)}(x_1,0) = \sigma_{22}^{(2)}(x_1,0) = \frac{4\mu}{\pi(\kappa+1)} \int_{-1}^{1} \frac{f(\xi)d\xi}{\xi-x_1} \quad . \tag{8.73}$$

If the crack is to be closed at both ends, the subsidiary condition

$$\int_{-1}^{1} f(\xi)d\xi = 0 \tag{8.74}$$

must be satisfied. A well known inversion formula for the integral equation (8.73) then gives

$$4\pi(1-x_1^2)^{\frac{1}{2}}f(x_1) = -\frac{(\kappa+1)}{\mu} \int_{-1}^{1} \frac{(1-\xi^2)^{\frac{1}{2}}}{(\xi-x_1)} t_2^{(2)}(\xi,0)d\xi + d \qquad \text{for } |x_1| < 1 \tag{8.75}$$

where d is an arbitrary constant to be determined from condition (8.74). Note that the above singular integrals are to be interpreted as their Cauchy principal values.

Since from the boundary condition (8.72)

$$t_2^{(2)}(\xi,0) = -t_2^{(1)}(\xi,0) \ , \qquad |\xi| < 1 \tag{8.76}$$

the integral equation (8.75) contains double integrals ($t_2^{(1)}(\xi,0) = \sigma_{22}^{(1)}(\xi,0)$ is given for the unflawed medium by an equation like equation (8.14) of the introduction). Rudolph and Ashbaugh [35] overcome this difficulty by changing the order of integration and evaluating various singular integrals analytically.

Finally the integral equations (8.13) and (8.75) are solved numerically for the unknown density $f(x_1)$, $-1 < x_1 < 1$ and the unknown $u_j(P)$ and $t_j(P)$ on corresponding parts of the boundary C. It should be noted that the efficacy of the procedure depends to a certain extent on quite a bit of subsidiary analytical work in reducing various double integrals to simple

ones. An alternative to the step from (8.73) to (8.75) would be to solve numerically the integral equation (8.73) directly with appropriate modelling of $f(\xi)$.

3.5 Crack modelling by Somigliana dislocations

A natural extension to the approach of the last section is to model the crack as a mosaic of infinitesimal dislocations of area dS_1, normal n_k and a discontinuity vector b_i which is effectively constant all over the small area dS_1. The displacement produced by one of these elementary dislocations can be written

$$du_j(\underset{\sim}{r}) = b_i n_k dS_1 p_{ik}^{(j)}(\underset{\sim}{r} - \underset{\sim}{r}') \tag{8.77}$$

where $p_{ik}^{(j)}(\underset{\sim}{r} - \underset{\sim}{r}')$ is the stress produced at a point $\underset{\sim}{r}'$ on S_1 by a point force of unit magnitude at $\underset{\sim}{r}$ parallel to the x_j axis and n_k is the normal to S_1 at $\underset{\sim}{r}'$. A Somigliana dislocation at S_1 (see Fig. 7) is characterised by the vector $\underset{\sim}{b}$ which is the displacement on the arrow side of S_1 defined by $\underset{\sim}{n}$, minus the value on the tail side of the arrow. Thus in an infinite linear elastic medium the displacement field due to the Somigliana dislocation can be shown to be

$$u_j(\underset{\sim}{r}) = \int_{S_1} b_i(\underset{\sim}{r}') p_{ik}^{(j)}(\underset{\sim}{r} - \underset{\sim}{r}')\, n_k dS_1 \tag{8.78}$$

Note that as far as the above formulation is concerned the surface S_1 can take any shape, so in principle a crack of any shape can be represented in this way. However, the numerical solution of the integral equation which results when expression (8.78) is differentiated to obtain the stress field requires further investigation. A proof of (8.78) which also verified its properties for an anisotropic medium was given by Burgers [37]. A derivation of (8.78) by means of the reciprocal theorem is attributed to Eshelby in

the book by Nabarro [38]. We shall give in the next section a derivation based on Betti's reciprocal theorem.

In principle the integral equation deduced from (8.78) by computing the stresses at $\underset{\sim}{r}$ and then letting $\underset{\sim}{r}$ tend to S_1 can be coupled with a boundary integral formulation of the external boundary in a similar manner to that of the last section. However, the numerical implementation of such a procedure has yet to be made. It should be noted nevertheless that this formulation can be used for any crack profile.

The special case of a flat crack in an infinite medium has been tackled by Weaver [39] using a formulation similar to that discussed above. He reduces the singular nature of the integral equations by first doing an integration by parts.

3.6 General formulation

We discuss here a general formulation of the crack problem in which the crack profile is modelled by a distribution of Somigliana dislocations. We begin with the formulation of the situation shown in Fig. 1 of section 1. If in equation (8.19) the external boundary S is allowed to tend to infinity and the boundary displacement and stresses are such that the integrals over S tend to zero, then since $\Sigma t_i(Q) = 0$ on Γ the following result is obtained:-

$$u_j(p) = - \int_{\Gamma} T_{ji}(p,Q)\Delta u_i(Q)dS(Q) \qquad (8.79)$$

It is easily seen that this result is equivalent to that of equation (8.78) by noting that $T_{ji} = -p_{ik}^{(j)}n_k$ if n_k is defined as in Fig. 7. Note that in the formulation of Weaver [39] where a crack with a flat three dimensional plan form is considered, the surface Γ is associated with the upper crack surface and hence has unit normal $n_i^+ = -\delta_{i3}$ in his notation, i.e. it is in

the opposite direction to that of Fig. 7. As indicated in the last section, the stresses can be computed from (8.79) by differentiating with respect to the point p.

In general for an internal crack such as shown in Fig. 1 we have (equation (8.19))

$$u_i(p) = -\int_S T_{ij}(p,Q)u_j(Q)dS(Q) + \int_S U_{ij}(p,Q)t_j(Q)dS(Q)$$

$$- \int_\Gamma T_{ij}(p,Q)\Delta u_j(Q)dS(Q) \qquad (8.80)$$

where $\Delta u_j(Q) = u_j(Q^+) - u_j(Q^-)$ and we have used the fact that $\Sigma t_j(Q) = t_j(Q^+) + t_j(Q^-) = 0$ across the crack. Differentiating (8.80) with respect to the co-ordinates of p to obtain the stresses gives

$$\sigma_{ij}(p) = \int_S D_{kij}(p,Q)t_k(Q)dS(Q) - \int_S S_{kij}(p,Q)u_k(Q)dS(Q)$$

$$- \int_\Gamma S_{kij}(p,Q)\Delta u_k(Q)dS(Q) \qquad (8.81)$$

The functions D_{kij} and S_{kij} are obtained by differentiating U_{ij} and T_{ij} respectively, the latter two functions can be deduced from equations (8.6) and (8.7) of the introduction.

There is no difficulty with the integral equation (8.80) as p tends to a boundary point P of S. The result is an integral equation like (8.80) with p replaced by P and $u_i(p)$ on the left hand side of (8.80) replaced by $u_i(P)/2$ (cf. equation (8.15) of the introduction). Thus for P belonging to S the usual boundary integral equation applies with the addition of a non-singular integral involving the unknown $\Delta u_j(Q)$. When p tends to a point of Γ, we have already seen in the introduction that the formulation (8.80) is inadequate. However, in our opinion, there is nothing wrong with an integral equation based on (8.81) for points p tending to P belonging to Γ.

The traction free (or stress free) boundary condition for a crack is sufficient to specify the integral equation for $\Delta u_k(Q)$, $Q \in \Gamma$.

The difficulty, of course, is in the implementation of this formulation. Nevertheless, we feel it should even be possible to deal numerically with the improper integrals resulting in (8.81) when $p \to P \in \Gamma$. Failing this, of course, it should be possible to integrate by parts in the integral over Γ in (8.81) before taking the limit $p \to P \in \Gamma$. This was done in [39] for the case of an infinite medium. Such a procedure does of course reduce the singular nature of the integrals and for two dimensional problems it leads to singular (Cauchy) integrals such as considered in section 3.4. This procedure is analogous to modelling the crack by extended dislocations (Volterra ones) as opposed to the infinitesimal Somigliana dislocations.

An integral equation formulation somewhat similar to that of (8.81) for the crack has been formulated and implemented by Montulli [40]. However, he uses such an integral equation together with a standard boundary integral equation along the crack surfaces. A somewhat similar procedure is being developed by Xanthis [41]. In either formulation we do not see that the extra equations are necessary, all that is required to model the crack, in our opinion, is the dislocation distribution. It should be stressed that the above formulation is intended as a general one to deal with any crack shape, the success or otherwise of this approach depends of course on the implementation. There are other methods which have been used in two dimensions to deal with notches and corners; we mention in this respect the work of Barone and Robinson [42]. Clearly more work is required before the definitive approach is determined.

4. Modelling and numerical results

We have indicated throughout the earlier sections, and in the introduction, that precise modelling of the crack tip singularity is essential to an accurate analysis of the fracture problem. In this section we give an account of some recent work (Xanthis et al [43]) which pays due attention to this singularity. The situation considered, that of anti-plane strain deformation (longitudinal shear), is perhaps the simplest in which this singular behavior can be exhibited. Nevertheless, the ideas discussed here should be of use in the more complicated problems discussed in section 3.

4.1 General formulation

Since anti-plane strain deformation is being considered there is only one non-zero displacement u and this acts perpendicular to the plane of the paper. The general problem is to determine u in a bounded open region Ω in R^2 with boundary $\partial\Omega$ where u satisfies the equations and boundary conditions:

$$\begin{aligned} \nabla^2 u &= 0 && \text{in } \Omega \\ u &= \bar{u} && \text{on } \partial\Omega_1 \\ \partial u/\partial n &= \bar{t} && \text{on } \partial\Omega_2 \\ \partial u/\partial n + \bar{c}u &= \bar{d} && \text{on } \partial\Omega_3 \end{aligned} \tag{8.82}$$

$\partial\Omega_1$, $\partial\Omega_2$ and $\partial\Omega_3$ are disjoint portions of the boundary with union equal to $\partial\Omega$ i.e. $\partial\Omega = \overline{\partial\Omega_1 \cup \partial\Omega_2 \cup \partial\Omega_3}$ and $\partial\Omega_i \cap \partial\Omega_j = \phi \quad i \neq j$. The expressions $\bar{u}$, $\bar{t}$, $\bar{c}$ and $\bar{d}$ are given functions and $\partial u/\partial n$ is the outward normal derivative of u). Since the displacement u satisfies Laplace's equation a scalar version of equation (8.15) can be derived via Green's third identity. The resulting integral equation on the boundary $\partial\Omega$ of the body is

$$\int T(P,Q)[u(Q) - u(P)]dS(Q) = \int U(P,Q) \frac{\partial u}{\partial n}(Q)dS(Q)$$

$$\text{for all } P \in \partial\Omega \,, \tag{8.83}$$

where

$$U(P,Q) \equiv (1/2\pi)\ln(1/r) \quad \text{with} \quad r = |P-Q|$$

$T(P,Q) \equiv \nabla_Q U(P,Q)\cdot \underline{n}(Q)$ where $\underline{n}.(Q)$ is the outward unit normal at the point $Q \in \partial\Omega$ and

$$\frac{\partial u(Q)}{\partial n} = \nabla u(Q) \,.\, \underline{n}(Q) \,.$$

For $Q \in \partial\Omega$ let

$$u^*(Q) \equiv u(Q), \qquad t^*(Q) \equiv \frac{\partial u}{\partial n}(Q)$$

then u^* and t^* satisfy

$$\int T(P,Q)[u^*(Q) - u^*(P)]dS(Q) = \int U(P,Q)t^*(Q)dS(Q)$$

$$\forall\ P \in \partial\Omega \tag{8.84}$$

$$\begin{aligned} u^*(P) &= \bar{u}(P) \qquad \forall\ P \in \partial\Omega_1 \\ t^*(P) &= \bar{t}(P) \qquad \forall\ P \in \partial\Omega_2 \end{aligned} \tag{8.85}$$

and

$$t^*(P) + \bar{c}(P)u^*(P) = \bar{d}(P) \qquad \forall\ P \in \partial\Omega_3 \,.$$

The object is thus to compute approximations $\tilde{u}$ and $\tilde{t}$ to u^* and t^* from the integral equation (8.83) and boundary conditions (8.85).

Any particular boundary element method is characterised by: (a) the choice of the classes of functions used to approximate u^* and t^*, and (b) the way in which the integral equation (8.83) is used in the determination of $\tilde{u}$ and $\tilde{t}$. In Xanthis et al [43] u^* and t^* are approximated by linear combinations of computationally convenient functions $v_\ell^{(u)}$, $\ell = 1,\ldots,n_1$, and $v_{\ell'}^{(t)}$, $\ell' = 1,\ldots,n_2$, respectively, i.e. one writes

$$\tilde{u} = \sum_{\ell=1}^{n_1} u_\ell v_\ell^{(u)}, \qquad \tilde{t} = \sum_{\ell'=1}^{n_2} t_{\ell'} v_{\ell'}^{(t)} \tag{8.86}$$

where the coefficients u_ℓ and $t_{\ell'}$ are determined so that with u^* and t^* in (8.84) replaced by $\tilde{u}$ and $\tilde{t}$, respectively, the integral equation is satisfied exactly at m boundary points $P^{(1)},\ldots,P^{(m)}$.

Thus, one obtains

$$\sum_{\ell=1}^{n_1} T_{k\ell} u_\ell = \sum_{\ell'=1}^{n_2} U_{k\ell'} t_{\ell'}, \qquad k = 1,\ldots,m \tag{8.87}$$

where

$$\begin{aligned} T_{k\ell} &\equiv \int T(P^{(k)},Q)[v_\ell^{(u)}(Q) - v_\ell^{(u)}(P)]dS(Q) \\ U_{k\ell'} &\equiv \int U(P^{(k)},Q)v_{\ell'}^{(t)}(Q)dS(Q) \end{aligned} \tag{8.88}$$

With an appropriate choice of m and the points $P^{(k)}$, by requiring that the boundary conditions (8.85) are satisfied exactly at $P^{(k)}$, $k = 1,\ldots,m$ and by imposing suitable continuity conditions (see 4.1.3) one arrives at n_1+n_2 equations for the n_1+n_2 unknowns u_ℓ and $t_{\ell'}$. Of course the success of the method depends in part on a sensible choice of the functions $v_\ell^{(u)}$ and $v_{\ell'}^{(t)}$ and they must be chosen so that u^* and t^* can be well approximated by linear combinations of them.

4.1.1 Approximation to the boundary

The following scheme is adopted for approximating the boundary: the boundary is subdivided into n 'elements' numbered in anti-clockwise order around the boundary, 1,...,n and on each element, e, there is chosen an internal node. The two element boundary nodes and the internal node are labeled in anti-clockwise order around the boundary $\partial\Omega$ as $P^{(e,1)}$, $P^{(e,2)}$

and $P^{(e,3)}$. The approximation to the part of the boundary passing through these nodes is specified by $P^{(e)}(\xi)$, $\xi \in [0,1]$ where

$$P^{(e)}(\xi) = \sum_{i=1}^{3} N_i^{(2)}(\xi) P^{(e,i)} \qquad (8.89)$$

with

$$N_1^{(2)}(\xi) = (1-\xi)(1-2\xi), \quad N_2^{(2)}(\xi) = 4\xi(1-\xi), \quad N_3^{(2)}(\xi) = \xi(2\xi-1)$$

The $N_i^{(2)}$, $i = 1,2,3$ are the quadratic Lagrange polynomials defined on $[0,1]$ with the property $N_i^{(2)}(\xi_j^{(2)}) = \delta_{ij}$ where $\xi_j^{(2)} = (j-1)/2$, $j = 1,2,3$.

More generally one can define $N_i^{(p)}$, $i = 1,\ldots,p+1$ to be the p^{th} order Lagrange polynomials with

$$N_i^{(p)}(\xi_j^{(p)}) = \delta_{ij}, \quad \xi_j^{(p)} = (j-1)/p, \qquad j = 1,\ldots,p+1.$$

For a good approximation to the boundary the element boundary nodes need to be chosen so that the portion of the boundary between them is smooth, hence corners of $\partial\Omega$ are chosen as element boundary nodes.

4.1.2 Choice of approximating functions

The functions $v^{(u)}$ and $v^{(t)}$ are chosen with the following considerations in mind: (i) u^* is continuous but t^* may have discontinuities, e.g. at corners or boundary points where there is a change in boundary condition type. Thus the $v^{(u)}$'s are chosen to be continuous and the $v^{(t)}$'s such that functions with discontinuities at selected boundary points can be represented accurately, (ii) the functions $v^{(u)}$ and $v^{(t)}$ must be computationally convenient.

It is assumed that the element nodes have been chosen so that the mapping (8.89) is invertible so an inverse mapping $\xi^{(e)}$ can be defined, i.e.

$$\xi = \xi^{(e)}(P^{(e)}(\xi)), \qquad \xi \in [0,1].$$

It is further assumed that every corner point of $\partial\Omega$ and every point of $\partial\Omega$ at which there is a change in boundary condition type is an element boundary node. Defining

$$N_i^{(e,p)}(P) \equiv N_i^{(p)}(\xi^{(e)}(P)), \quad \forall\, P \in \{P : P = P^{(e)}(\xi), \quad \xi \in [0,1] \qquad (8.90)$$

it follows that

$$\sum_{i=1}^{p+1} N_i^{(e,p)}(P) = 1$$

and

$$N_i^{(e,p)}(P^{(e,p,j)}) = \delta_{ij}$$

where

$$P^{(e,p,j)} \equiv (P^{(e)}(\xi^{(p,j)}) \text{ with } \xi^{(p,j)} \equiv (j-1)/p, \quad j = 1,\ldots,p+1.$$

The set of nodes $P^{(e,p,j)}$, $j = 1,\ldots,p+1$ consists of the end point nodes of the element e and p-1 internal nodes.

Let the set of all end point and internal nodes $P^{(e,p,j)}$, be numbered, in, say, anticlockwise order around $\partial\Omega$, $1,\ldots,np$ (see fig. 8), and let the coordinates of the ℓth node be denoted by $P^{(\ell)}$. Thus $P^{(e,p,j)} = P^{(\ell)}$ when

$$\ell = \ell(e,j) \equiv (e-1)\cdot p + j.$$

The functions $v^{(u)}$ and $v^{(t)}$ are defined in terms of the functions $N^{(e,p)}$ in the following way:

Take n_1 (the number of $v^{(u)}$ functions) to be $n \cdot p$ and define

$$v_\ell^{(u)}(P) = \begin{cases} 0, & \text{unless P belongs to an element having } \ell \text{ as a node.} \\ N_j^{(e,p)}(P), & \text{when } \ell \text{ is the jth node of e and } P \in e. \end{cases} \qquad (8.91)$$

Take n_2 (the number of $v^{(t)}$ functions) to be $n\cdot(p+1)$ and associate each $v^{(t)}$ function with an element and a node belonging to the element.

$$v^{(t)}_{\ell'}(P) = v^{(t)}_{\ell'(e,j)}(P) = \begin{cases} 0, & \text{unless } P \in e, \\ N^{(e,P)}_j(P), & \text{when } P \in e, \end{cases} \tag{8.92}$$

where $\ell'(e,j) \equiv (e-1)\cdot(p+1) + j$. Note that the novelty of defining the $v^{(t)}_{\ell'}$ functions this way represents an accurate modelling technique of the 'corner-problem' (Fig. 9) which does not require the equality of the tractions $t_i^{(1)}$ and $t_i^{(2)}$ on an interelement corner node (note that Lachat [44] and Lachat and Watson [45] assume $t_i^{(1)} = t_i^{(2)}$).

It follows from these definitions that

$$\begin{aligned} &v^{(u)} \text{ is continuous,} \\ &v^{(u)}_k(P^{(\ell)}) = \delta_{k\ell}, \\ &\sum_{\ell} v^{(u)}_{\ell}(P) = 1 . \end{aligned} \tag{8.93}$$

It follows also that $v^{(u)}_{\ell}$ is zero except on the element (or elements) having ℓ as a node, that $v^{(t)}_{\ell'(e,j)}$ is zero except on element e and that, when $\ell'(e,j)$ is an interelement node, i.e. $j = 1$, or $p+1$, then $v^{(t)}_{\ell'(e,j)}$ is discontinuous at the node $\ell'(e,j)$.

With these choices of $v^{(u)}$ and $v^{(t)}$ the total number of unknowns u_{ℓ} and t_{ℓ}, is $n\cdot p+n(p+1)$. The set of points at which the integral equation is to be satisfied is taken as the $m = n\cdot p$ boundary nodes $P^{(1)},\ldots,P^{(m)}$ (c.f. eq. (8.87)). By imposing the boundary conditions at these nodes and, where appropriate, continuity conditions on t at interelement nodes, as many (linear) equations as there are unknowns are obtained.

4.1.3 Boundary and continuity conditions

The interelement nodes are chosen so that any point on the boundary at which the boundary condition type changes is an interelement node. At every node internal to an element it is required that the boundary condition be satisfied. At every interelement node the boundary conditions associated with each of the elements having the interelement node in common are to be satisfied. Thus there is associated with each internal node two unknowns (one u_ℓ and one t_ℓ, coefficient) and two equations - one associated with the integral equation and one with the boundary condition. At an interelement node there are associated three unknowns (one u_ℓ and two t_ℓ, coefficients) and, in general, three equations - one associated with the integral equation and two with the boundary conditions.

The exceptional case arises when the node is an interelement node between two nodes which are both of Dirichlet type, when the imposition of the boundary conditions provides only one equation. If the boundary is smooth at such an interelement node we require, in addition, that $\tilde{t}$ be continuous (and hence the two t_ℓ, coefficients associated with the node be equal) thus providing one additional equation. If the interelement node is a corner node, then from the directional derivatives of u along the two tangents at the node the gradient and hence normal derivatives of u can be computed. In this case, then, the boundary conditions determine the values of the three unknowns associated with the node and we simply exclude from our final set of equations the integral equation associated with the node.

In summary, there are sets of equations associated with

(a) the integral equation,

(b) the boundary conditions, and

(c) the continuity of the normal derivative,

and there are as many of these equations as there are unknowns.

The contribution from element e to $U_{k\ell(e,j)}$ is

$$\int_0^1 U(P^{(k)}, P^{(e)}(\xi))N_j^{(p)}(\xi)\,\frac{ds}{d\xi}(\xi)\,d\xi$$

and, since $v_k^{(u)}(P^{(\ell)}) = \delta_{k\ell}$, the contribution from element e to $T_{k\ell(e,j)}$ for $\ell(e,j) \neq k$, is

$$\int_0^1 T(P^{(k)}, P^{(e)}(\xi))N_j^{(p)}(\xi)\,\frac{ds}{d\xi}(\xi)d\xi,$$

where

$$\frac{ds}{d\xi} = \left|\frac{dP^{(e)}}{d\xi}(\xi)\right|.$$

In both cases the integrals can be evaluated accurately using appropriate gaussian quadrature schemes. An immediate consequence of (8.93) is that with u_ℓ = const. and $t_{\ell'} = 0$, $\tilde{u}$ and $\tilde{t}$ provide an exact solution of the integral equation (8.84). Thus from (8.87) it follows that

$$\sum_\ell T_{k\ell} = 0$$

and thus T_{kk} can be computed as

$$-\sum_{\ell\neq k} T_{k\ell}.$$

The boundary and continuity conditions are used to eliminate variables as the assembly progresses so that when assembly is completed, a system of m equations for the m unknowns is obtained. When these have been solved the remaining unknowns are computed.

4.2 Treatment of singularities

4.2.1 Singularities in a model problem

In [43] the following model problem is considered:

Find u such that

$$\nabla^2 u = 0$$

in the 14×14 square region EFGH, in which there is a slit (crack) OA joining the centre of the square O (the crack tip) to the midside A of EH (see fig. 10) with

$u = 0$ on HA

$u = 1000$ on AE,

and $\partial u/\partial n = 0$ on the remaining boundary.

By symmetry u-500 is antisymmetric about the line AB and in the rectangular region EFBOA u is the solution of the 'model problem'

(Fig. 10 here)

$\nabla^2 u = 0$ in EFBOA

$u = 1000$ on AE

$u = 500$ on BO

$\partial u/\partial n = 0$ on OA, EF and FB

Using the standard separation of variables technique, the boundary conditions on OA, the boundedness and anti-symmetry of u - 500, one obtains (see e.g. [46])

$$u(P) = u(O) + \sum_{j=0}^{\infty} \alpha_j f_j(r,\theta) \qquad (8.94)$$

in the neighbourhood of O, and, hence, for P on OB,

$$\frac{\partial u}{\partial n} = \sum_{j=0}^{\infty} \alpha_j \frac{1}{r} \frac{\partial f_j}{\partial \theta}(r,0), \qquad (8.95)$$

where

$$f_j(r,\theta) \equiv r^{(2j+1)/2} \sin\{(\tfrac{2j+1}{2})\theta\}$$

and (r,θ) are the polar coordinates of P.

In problems of this kind the coefficient, α_0, of the leading term, is of special interest, e.g. in the crack problem the corresponding coefficient is proportional to the stress intensity factor (SIF). Note that, for the model problem we have

$$\alpha_0 = \begin{cases} \lim_{r\to 0} r^{-\frac{1}{2}}[u(r,\pi) - u(0,0)], & (8.96) \\ \lim_{r\to 0} 2r^{\frac{1}{2}} \frac{\partial u}{\partial n}(r,0). & (8.97) \end{cases}$$

The boundary element method as described in section (4.1) is now applied to this model problem. Let the boundary of the region, EFBOA, be subdivided into n elements and let the elements be numbered anticlockwise from O as shown in Fig. 11a.

Since on OB, in the neighbourhood of O, t* behaves like $r^{-1/2}$, while $\tilde{t}$ is bounded, we cannot expect to obtain an accurate representation of t* near O. On OA, in the neighbourhood of O, u* behaves like $r^{1/2}$, while on element 1, if the internal node $P^{(1,2)}$ is chosen to be mid-way between the element boundary nodes, and p is taken to be 2, $\tilde{u}$ will be a quadratic function of r and hence cannot accurately represent u*.

Thus we would not expect the method of section 4.1 to work well for this problem and in particular we would expect poor results for the computed values of α_0. In this section we describe various ways of overcoming these difficulties and in section 4.3 we attempt to compare their efficacy. Some of the techniques can be extended in a natural way to deal with singularities in more general problems for which the form of the singularity is known. While techniques of the kind described here have

been used in standard finite element method calculations of stress intensity factors (SIF) for crack problems, the use of some of them in the BIE context appears to be new. In the standard FE method calculations of SIF's basically three types of methods have been used:

(1) Those methods which use special functions having the correct singular behaviour in the neighbourhood of the singularity (see sections 4.2.2, 4.2.3). For the BIE such special functions can be introduced by modifying the definitions of $v^{(t)}$ and $v^{(u)}$ of section 4.1 to include functions having the correct singular behaviour. For $v^{(u)}$, an elegant alternative is to choose element internal nodes, $P^{(e,2)}$, so that $v^{(u)}$ has the $r^{1/2}$ behaviour of u.

(2) Those methods which transform the problem into one in which singularities are not present. Two such methods are:

(a) subtraction of singularity techniques (see section 4.2.4), and

(b) conformal mapping techniques. This technique has been used successfully for problems in two dimensions (see e.g. [47]). However, since it cannot be extended to deal with problems in three dimensions it is excluded from our discussion.

(3) Those methods which do not use special functions but employ fine meshes near to the singularity.

From a computed solution obtained by whatever method, one can compute approximations to α_0 by a variety of schemes (see section 4.3). If the solution is calculated by a given method, for a succession of grid refinements, then 'extrapolation to zero grid size' of the values of α_0 computed by one such scheme, may yield an excellent approximation to α_0; see e.g. Morley [48] where extrapolation leads to a considerably improved approximation.

Extrapolation techniques will give good results when (i) the error, e(h), in the computed value of α_0 behaves asymptotically like some power of h, where h is a measure of fineness of the grid, and (ii) the computations

are carried out for values of h for which e(h) is well approximated by its asymptotic form. When condition (i) holds one would expect that grids for which e(h) has this property will be relatively much coarser for those methods for solving boundary value problems in which special provision is made for treating singularities, than in those methods in which no such provision is made.

4.2.2 Treatment of singularities in u^* and t^* using special functions

(A). A treatment of the $r^{-1/2}$ singularity in t^* using special functions

Suppose that we wish to represent the $r^{-1/2}$ behaviour over an interval OB' where B' lies on the interval OB. The element subdivision is chosen so that B' is an interelement node and, for each element belonging to OB', the internal element nodes $P^{(e,2)}$ are taken to be mid-way between the element boundary nodes $P^{(e,1)}$ and $P^{(e,3)}$ so that

$$P^{(e)}(\xi) = P^{(e,1)} + \xi(P^{(e,3)} - P^{(e,1)}).$$

Let the length of the element e be $\ell^{(e)}$ and let the radial coordinates of B', $P^{(e,1)}$ and $P^{(e)}(\xi)$ be $r_{B'}$, $d^{(e)}$ and $r^{(e)}(\xi)$, respectively (see fig. 11(b)). Thus for $\xi \in [0,1]$

$$r^{(e)}(\xi) = \ell^{(e)}(\lambda^{(e)} - \xi),$$

where

$$\lambda^{(e)} \equiv d^{(e)}/\ell^{(e)}.$$

We define $v^{(t)}_{\ell'(e,j)}$ as in section 4.1.2 except that, for $e \in OB'$, we replace $N^{(p)}_i$ in the definition (8.89) by $N^{(p,e)}_i$ where

$$N^{(p,e)}_i(\xi) \equiv (r_B/r^{(e)}(\xi))^{1/2} N^{(p)}_i(\xi).$$

Thus, this definition of $v^{(t)}_{\ell'(e,j)}$ differs from that given in section 4.1.2 only when e $\in$ OB'. Note that the interelement continuity between singular/continuation/ordinary boundary elements is preserved. (Fig. 11(c)).

It follows at once from this definition that, for every set of coefficients $t_{\ell'(e,j)}$ for which the continuity conditions of section 4.1.3 are satisfied, on OB', $\tilde{t}(P)$ has the form $P_1(r)r^{-1/2}$, where $(r,0)$ are the polar coordinates of the point P, $P_1(r)$ is continuous and is a pth degree polynomial on each element e; conversely, to every such function $P_1(r)$ there corresponds a set of coefficients $t_{\ell'(e,j)}$ such that $\tilde{t}$ has the form $P_1(r)r^{-1/2}$. Thus, using these singular $v^{(t)}$ functions we can accurately represent the sum of the first (p+1) terms in the expansion (8.95) for t^* on OB'.

(B) <u>A treatment of the $r^{1/2}$ singularity in u^* using special functions</u>

Let the internal node $P^{(1,2)}$ of element 1 be mid-way between the element boundary nodes $P^{(1,1)}$ and $P^{(1,3)}$ and let the functions $\hat{N}^{(p)}_i(\xi)$ be defined by

$$\hat{N}^{(p)}_i(\xi) = [\xi^{(p)}_i/\xi]^{1/2} N^{(p)}_i(\xi), \qquad i = 2,\ldots,p+1$$

$$\hat{N}^{(p)}_1(\xi) = 1 - \sum_{i=2}^{p+1} N^{(p)}_i(\xi) .$$

We define $v^{(u)}_\ell$ as in section 4.1.2 but with $N^{(p)}_i(\xi)$ replaced by $\hat{N}^{(p)}_i(\xi)$ when e = 1. Note that in this definition the $v^{(u)}_\ell$ retain the properties (8.93). It follows from this definition that, on element 1, u has the form

$$\tilde{u}(P) = u(0) + r^{1/2} Q_1(r)$$

where r is the radial coordinate of the point P and $Q_1(r)$ is a (p-1)th degree polynomial in r. Thus, using the functions $v^{(u)}_\ell$, defined in this way, $\tilde{u}$ can accurately represent the sum of the first p terms in the

expansion (8.94) for u^*, on the element 1. Unfortunately, there does not seem to be any simple way of introducing special functions, $\hat{N}$, for elements 2,3,..., to reproduce the $r^{1/2}$ behaviour over those elements while retaining the property (8.93).

4.2.3 Treatment of the $r^{1/2}$ singularity in u using the element parametrization

An alternative way of treating the $r^{1/2}$ singularity in u which does not involve the introduction of special $v^{(u)}$ functions was suggested by a device originally proposed independently by Barsoum [49] and Henshell and Shaw [50] and extended by Lynn and Ingraffea [51] in the context of the finite element method.

Consider a typical element e of length 2h on OA as shown in fig. 12. Let the distance of $P^{(e,2)}$ from $P^{(e,1)}$ be $p^{(e)}h$ and the distance of $P^{(e,1)}$ from the point O be $q^{(e)}h$. Let r be the polar coordinate of the point $P^{(e)}(\xi)$ and let the position of the internal node $P^{(e,2)}$ be chosen so that

$$p^{(e)} = \frac{1}{2}\left(1-q^{(e)} + \sqrt{q^{(e)}(q^{(e)} + 2)}\right) , \tag{8.98}$$

then

$$\xi = Q_1(q^{(e)})\{1 - \sqrt{r/(q^{(e)}h)}\} ,$$

where

$$Q_1(q) = 1/\{1 - \sqrt{(q+2)/q}\}$$

and hence $\tilde{u}$ will be a pth degree polynomial in $r^{1/2}$ on the element e. Thus if the position of the internal nodes of the elements 1,2,..., belonging to OA are chosen according to (8.98), then $\tilde{u}$ can accurately represent any continuous function which is piecewise a pth degree polynomial in $r^{1/2}$ on those elements. In particular, taking p = 1, $\tilde{u}$ can accurately represent any function of the form

$$u(0) + \beta_1 r^{1/2} \quad .$$

Thus, using this scheme, with p = 1, we can reproduce the first term in the expansion (8.94) for u near 0.

Unfortunately, to reproduce the first q terms in the expansion, we must take p = 2q - 1.

In the boundary element method described in section 4.1 the boundary of the region is approximated by a curve which is defined parametrically in terms of quadratic Lagrangian interpolation polynomials. An obvious generalization of this specification of the boundary is obtained by taking m > 1 internal nodes per element and using (m+1)th order Lagrangian polynomials in the parametric definition of the boundary. Pu, Hussain and Lorensen [52] have extended the work of [49] and [50] to the case m = 2. They give formulae for the position of the two internal nodes on element 1 such that ξ is linear in $r^{1/2}$ on the element. Bernal and Xanthis [53] have derived formulae for the position of the two internal nodes on any element belonging to OA, such that ξ is linear in $r^{1/2}$ on all elements $e \in OA$. For the case m = 2, with this choice of internal nodes, $v^{(u)}$, as defined by (8.91), has the desired $r^{1/2}$ behaviour. However, results are presented for the case r = 2, p = 2 only. In summary, we can introduce the $r^{-1/2}$ behaviour of t^* into $\tilde{t}$ by using the modified Lagrangian interpolation functions, $\hat{N}_i^{(p,e)}$, and the $r^{1/2}$ behaviour of u^* into $\tilde{u}$ by using the modified Lagrangian functions, $\hat{N}_i^{(p)}$, or, for the case p = 2, by choosing the internal element nodes, $P^{(e,2)}$, (for e = 1,2,..., and $e \in OA$) according to (8.98). An alternative way of treating the singularity is to transform the problem, using a subtraction of singularity technique, so that the solution of the transformed problem, to be solved by the BIE method, does not possess singularities.

4.2.4 Subtraction of singularities

In the neighbourhood of O

$$u(r,\theta) = u(0) + \sum_{j=0}^{\infty} \alpha_j f_j(r,\theta),$$

where

$$f_j(r,\theta) = r^{(2j+1)/2} \sin\{\tfrac{1}{2}(2j+1)\theta\}$$

Thus we might reasonably expect that, near O, u could be approximated closely by retaining only a few (say, q+1) terms of the sum, i.e. that

$$u \simeq u(0) + \sum_{j=0}^{q} \alpha_j f_j \quad , \quad \text{near O.}$$

Let us define

$$\psi^{(q)} = u - \sum_{j=0}^{q} \alpha_j f_j \ , \tag{8.99}$$

then,

(i) if $\psi^{(q)}$ were known we could compute u at once from (8.99),

(ii) since the f_j are harmonic functions, $\psi^{(q)}$ is the solution of the boundary value problem:

$P_1^{(q)}$: find $\psi^{(q)}$ such that $\nabla^2\psi^{(q)} = 0$ in EFBOA,

$$\psi^{(q)} = \begin{cases} 1000 - \sum_{j=0}^{q} \alpha_j f_j & \text{on AE,} \\ 500 - \sum_{j=0}^{q} \alpha_j f_j & \text{on BO,} \end{cases}$$

$$\frac{\partial\psi^{(q)}}{\partial n} = - \sum_{j=0}^{q} \alpha_j \frac{\partial f_j}{\partial n} \quad \text{on OA, EF and FB,}$$

(iii) whereas u has discontinuous derivatives at 0, $\psi^{(q)}$ has continuous derivatives of order q.

Any numerical scheme for computing an approximation $\tilde{\psi}^{(q)} \approx \psi^{(q)}$ provides an approximation $\tilde{u}^{(q)}$ to u:

$$\tilde{u}^{(q)} = \tilde{\psi}^{(q)} + \sum_{j=0}^{q} \alpha_j f_j$$

and by virtue of (iii) we might expect that an algorithm (e.g. finite difference, finite element, BIE method) in which no special steps are taken to treat singularities, would consequently give a reasonable approximation $\tilde{\psi}(q)$ to the solution $\psi^{(q)}$ of $P_1{}^{(q)}$, and hence that $\tilde{u}^{(q)}$, defined by (8.99), would give a reasonable approximation to u.

Of course, to use such an approach we would have to know $\alpha_0,\ldots,\alpha_q$, or at least be able to determine sufficiently good approximations to these constants. Thus the equations derived from whatever scheme we use (FD, FE, etc.) must be supplemented by additional equations such that the total system of equations determines simultaneously an approximation $\tilde{\psi}^{(q)}$ to $\psi^{(q)}$ and approximations $\tilde{\alpha}_j^{(q)}$ to α_j $(j = 0,\ldots,q)$. Since, as we have already noted,

$$u \approx u(0) + \sum_{j=0}^{q} \alpha_j f_j, \qquad \text{near } 0,$$

we might take, in the case of finite difference or finite element schemes, the additional equations to be, for example, those obtained from the requirement

$$\tilde{\psi}^{(q)} = u(0),$$

at (q+1) nodes near 0, not belonging to that part $(\partial\Omega_1)$ of the boundary $(\partial\Omega)$ on which u is prescribed.

In the case of the BIE method described in section 4.1 with the approximations,

$$\tilde{\psi}^{(q)*} = \Sigma \psi_{\ell} v_{\ell}^{(u)}, \qquad \tilde{\chi}^{(q)*} = \Sigma \chi_{\ell'} v_{\ell'}^{(t)}$$

to $\psi^{(q)*}$ and $\chi^{(q)*} \equiv \partial\psi^{(q)}/\partial n$, respectively, we might take as additional equations those obtained from the requirement that $\tilde{\chi}^{(q)*}$ be continuous at 0, $\tilde{\psi}^{(q)*} = u(0)$ at r_1 points of $\partial\Omega$ near 0, not on $\partial\Omega_1$, and $\tilde{\chi}^{(q)*} = 0$ at r_2 points of $\partial\Omega$ near 0 and not on that part, $\partial\Omega_2$, of the boundary on which $\partial u/\partial n$ is prescribed, where $r_1+r_2 = q$.

Thus, with elements numbered as in fig. 11, and with $p = 2$, we might, for example, take

$$\chi_{(n,3)} = 0 \quad \text{if } q = 0,$$

and additionally

$$\chi_{(n,2)} = 0, \quad \psi_2 = u(0) \quad \text{if } q = 2,$$

and additionally

$$\chi_{(n,1)} = 0, \quad \psi_3 = u(0) \quad \text{if } q = 4.$$

The subtraction method outlined above can easily be extended to deal with any problem for which the form of the singularity is known (e.g. any reentrant corner problem). Symm [54] was, perhaps, the first to use this technique in the context of integral equations (his approximating functions $v^{(u)}$ and $v^{(t)}$ were step functions). See also Papamichael and Symm [55] where the work of [54] is amplified. Xanthis et al [43] have used the subtraction of singularity technique with both the finite difference method and the BIE method described in section 4.1. In both cases the method worked well. Their BIE calculations are reported in the following section.

The program for computing the coefficients ψ_ℓ and $\chi_{\ell,1}$ and the coefficients $\tilde{\alpha}_j$, $j = 0,\ldots,q$, by the BIE method, was obtained by a relatively trivial modification of the program described briefly at the end of section 4.1.

4.3 Numerical results for the model problem

In [43], the basic BIE method described in section 4.1 and modifications of this method, using the techniques described in section 4.2 have been used to compute solutions of the model problem given in Fig. 10, of section 4.2.1.

Each of the five boundary segments OA, AE, EF, FB and BC were subdivided into N elements of equal length, and for N = 2, 3, 4 and 5 the solution of the model problem was computed by each of the following modifications of the basic method described in section 4.1:

Method 1. No modification.

Method 2. $v^{(u)}$ functions with $r^{1/2}$ behaviour on element 1 (section 4.2): $v^{(t)}$ functions with $r^{-1/2}$ behaviour on OB (sections 4.2.2).

Method 3, nodes on OA chosen so that $v^{(u)}$ has $r^{1/2}$ behaviour on OA (section 4.3); $v^{(t)}$ as in Method 2.

Method 4, subtraction of singularity technique (section 4.2.4). For this method the computations were carried out for q = 0, 2 and 4.

For each computed solution, the values of u at the points (r,π), r = 1/4 and r = 3/4, were calculated.

4.3.1 Computed u values

These are given in tables 1a and 1b. From these tables it is evident that, for a given value of N, method 4 with q = 4 gives the most accurate results; method 2 and method 4 with q = 2 give results which are nearly as accurate as those obtained from method 4 with q = 4. However, this conclusion does not imply that α_0, the parameter which is usually of most importance in the applications, would also be given most accurately by method 4.

Table 1a

Values of u at r = 1/4; 'exact' value = 576.41 [54]

Method	1	2	3	4		
N				q = 0	q = 2	q = 4
2	534.17	576.22	574.79	576.51	576.48	576.44
3	540.69	576.31	575.69	576.48	576.42	576.41
4	545.96	576.36	576.06	576.47	576.41	576.41
5	550.38	576.38	576.25	576.42	576.41	576.41

Table 1b

Values of u at r = 3/4; 'exact' value = 634.45 [54]

Method	1	2	3	4		
N				q = 0	q = 2	q = 4
2	596.96	634.29	634.15	634.68	634.56	634.50
3	611.49	634.40	634.77	634.50	634.46	634.45
4	621.29	634.44	634.88	634.43	634.45	634.45
5	627.70	634.45	634.85	634.45	634.45	634.45

4.3.2 Calculation of an approximation $\hat{\alpha}_0$ to α_0

For Method 4, above, we can take $\hat{\alpha}_0 = \tilde{\alpha}_0$. By whatever method $\tilde{u}$ and $\tilde{t}$ are computed, one can use the formulae obtained by substituting $\tilde{u}$ and $\tilde{t}$ into the r.h.s. of (8.96) and (8.97), respectively, to obtain approximations to α_0:

$$\hat{\alpha}_0 = \alpha_0^{(u)}(\tilde{u}) \equiv \lim_{r\to 0} r^{-1/2}[\tilde{u}(r,\pi) - \tilde{u}(0)] \qquad (8.96)_a$$

and

$$\hat{\alpha}_0 = \alpha_0^{(t)}(\tilde{t}) \equiv \lim_{r\to 0} 2r^{1/2}\tilde{t}(r,0). \qquad (8.97)_a$$

Note that if $\tilde{u}$ and $\tilde{t}$ are obtained from

(i) Method 4, then

$$\alpha_0^{(u)}(\tilde{u}) = \alpha_0^{(t)}(\tilde{t}) = \tilde{\alpha}_0.$$

(ii) Method 1, then

$$\hat{\alpha}_0^{(u)}(\tilde{u}) = \alpha_0^{(t)}(\tilde{t}) = 0.$$

Nevertheless, in case (ii), one can obtain useful approximations to α_0 from $\tilde{u}$ and $\tilde{t}$ using the approximations to (8.96) and (8.97):

$$\hat{\alpha}_0^{(u)}(\tilde{u},r_u) = r_u^{-1/2}[\tilde{u}(r_u,\pi) - \tilde{u}(0)] \qquad (8.96)_b$$

and

$$\hat{\alpha}_0^{(t)}(\tilde{t},r_t) = 2r_t^{1/2}\tilde{t}(r_t,0) \qquad (8.97)_b$$

with r_u, r_t sufficiently small. Formulae $(8.96)_b$ and $(8.97)_b$ can, of course, be used to compute approximations to α_0 however $\tilde{u}$ and $\tilde{t}$ are calculated. For Method 1, experiments showed that there exist constants a, v, a*, v* such that, with

$$r_u = a\ell^v, \qquad r_1 = a^*\ell^{v^*},$$

(where ℓ = length of element 1 = length of element n = 7/N), $\hat{\alpha}^{(u)}(\tilde{u}, r_u)$ and $\hat{\alpha}^{(t)}(\tilde{t}, r_t)$ approximate closely α_0. The attempt to determine such constants was prompted by the observation of Schatz and Wahlbin [56] that, for the standard finite element method, a good choice of r for $\alpha_0^{(u)}$ is $h^{2/3}$ where h is the maximum diameter of all elements. The fact that we were able to find constants a, v, a*, v* so that α_0 is closely approximated by $\hat{\alpha}_0^{(u)}(\tilde{u}, r_u)$ and $\hat{\alpha}_0^{(t)}(\tilde{t}, r_t)$ is obviously significant and this is currently being investigated. Additional approximations to α_0 can be obtained from formulae deduced from certain path-independent (invariant) integrals, the F- and M-integrals, evaluated along a circuit surrounding the point where the singularity occurs (see section 2.2). These integrals are defined by

$$F_\ell = \int_S P_{j\ell} n_j \, dS, \tag{8.100}$$

$$M = \int_S x_t P_{jt} n_j \, dS, \tag{8.101}$$

where S is a plane curve with normal $n = (n_1, n_2)$, $P_{j\ell}$ the energy-momentum tensor

$$P_{j\ell} = L\delta_{\ell j} - \frac{\partial L}{\partial u_{,j}} u_{,\ell}$$

and L, the Lagrangian function, $L = \frac{1}{2}(u_{,1}^2 + u_{,2}^2)$.

Taking the x_2-axis to be along AB and S to be a closed path containing the point O - the crack tip (see fig. 10) - one obtains

$$F_2 = \pi\alpha_0^2/2, \tag{8.102}$$

$$M = \alpha\pi\alpha_0^2/2. \tag{8.103}$$

In particular, taking S to be the square EFGH and using the symmetry properties of the integrals and the computed $\tilde{u}$ and $\tilde{t}$ values, one can find approximations $\tilde{F}_2$ and $\tilde{M}$ to F_2 and M, and, hence, approximations to α_0 from (8.102) and (8.103), which are denoted by $\hat{\alpha}_0^{(F)}(\tilde{u},\tilde{t})$ and $\hat{\alpha}_0^{(M)}(\tilde{u},\tilde{t})$ respectively.

From the $\tilde{u}$ and $\tilde{t}$ values, computed by the four BIE variants, Methods 1, 2, 3 and 4, approximations to α_0 are calculated and the results given in the following tables.

Inspection of table 2b, c, d and e, shows that for the Methods 2, 3 and 4 one can obtain very accurate values for α_0, with a coarse grid (N = 2,3,4), using the approximations $\hat{\alpha}_0^{(F)}(\tilde{u},\tilde{t})$, $\hat{\alpha}_0^{(t)}(\tilde{t})$ and, for Method 4, $\bar{\alpha}_0$. For Method 1 to give an approximation to α_0 using $\hat{\alpha}_0^{(F)}(\tilde{u},\tilde{t})$ or $\hat{\alpha}_0^{(M)}(\tilde{u},\tilde{t})$, to an accuracy comparable to that obtained from Methods 2, 3 and 4 with a coarse grid (N $\simeq$ 5), a much finer grid must be used. For example, N = 10 gives $\hat{\alpha}_0^{(F)}(\tilde{u},\tilde{t})$ = 151.41 and $\hat{\alpha}_0^{(M)}(\tilde{u},\tilde{t})$ = 151.76, values which are not as accurate as those obtained by the other methods with N = 5. Nevertheless, the values $\hat{\alpha}_0^{(F)}(\tilde{u},\tilde{t})$ and $\hat{\alpha}_0^{(M)}(\tilde{u},\tilde{t})$ obtained using Method 1 with N = 5 are accurate to approximately one per cent. Perhaps it is worth noting that (i) $\hat{\alpha}_0^{(t)}(\tilde{t})$ is obtained as a simple multiple of one of the unknowns, whereas $\hat{\alpha}_0^{(F)}(\tilde{u},\tilde{t})$ and $\hat{\alpha}_0^{(M)}(\tilde{u},\tilde{t})$ involve the computation of line integrals, and (ii) Method 4 gives $\bar{\alpha}_0$ without any further computations, although it must be remembered that the system of equations from which the solution is obtained involves q+1 more equations than the other methods. Extrapolation to zero grid size, for $\hat{\alpha}_0^{(u)}(\tilde{u})$, was carried out by assuming that

$$\hat{\alpha}_0^{(u)} = \alpha_0 + A(1/N)^{\beta} ,$$

the constants α_0, A and β in this formula being determined from the values of $\hat{\alpha}_0(\tilde{u})$ for three successive values of N. For method 2, using N = 2,3,4

and N = 3,4,5, the computed values of α_0 were 151.78 and 151.64 respectively. For Method 3 the corresponding results were 151.58 and 151.64, respectively. These results demonstrate clearly the benefits of extrapolation.

4.4 Concluding remarks

An improved implementation of the BIE method has been discussed, which provides a special treatment of discontinuities associated with corners and points at which there is a discontinuity in the boundary condition. Three variants of this basic algorithm have been introduced with modifications capable of accommodating boundary singularities.

It must be noted that, although one boundary singularity has been considered, any number of such singularities may be treated simultaneously. The same treatment of the square-root singularity that has been described in the context of harmonic problems is directly applicable (component wise) to similar situations involving Navier's equation of elasticity. An attractive feature in the three methods described in section 4 is that the stress intensity factor appears as one of the unknowns in the computation or a simple linear combination of these unknowns, thus avoiding the uncertainties associated with schemes which involve plotting and extrapolation techniques.

In addition to the improved implementation the results of [43] show how the invariant integrals of section 2.2 can be used both directly and as a check on other methods of stress intensity factor determination. These methods have also been applied to certain crack problems in elastic media with spatially varying elastic properties [57].

Table 2

Computed α_0 values by three BIE variants. For Method 4 higher order coefficients for α_j are also presented. 'Exact' value of α_0 = 151.63 [54]

	N	2	3	4	5	
Method 1	$\alpha_0^{(F)}(u,t)$	155.52	154.22	153.57	153.18	(a)
	$\alpha_0^{(M)}(u,t)$	152.29	152.07	151.96	151.89	

	N	$\alpha_0^{(u)}(\bar{u})$	$\alpha_0^{(t)}(\bar{t})$	$\alpha_0^{(F)}(\bar{u},\bar{u})$	$\alpha_0^{(M)}(\bar{u},\bar{t})$	
Method 2	2	151.13	151.74	151.66	151.57	(b)
	3	151.35	151.65	151.63	151.62	
	4	151.46	151.63	151.63	151.62	
	5	151.51	151.63	151.63	151.62	

	N	$\alpha_0^{(u)}(\bar{u})$	$\alpha_0^{(t)}(\bar{t})$	$\alpha_0^{(F)}(\bar{u},\bar{t})$	$\alpha_0^{(M)}(\bar{u},\bar{t})$	
Method 3	2	142.32	151.72	151.66	151.56	(c)
	3	145.58	151.64	151.63	151.61	
	4	147.17	151.63	151.63	151.62	
	5	148.11	151.63	151.63	151.62	

	N	q	α_0	q	α_0	α_1	α_2	
Method 4	2	0	150.56	2	151.71	4.68	0.13931	(d)
	3		150.86		151.63	4.71	0.13838	
	4		151.05		151.63	4.72	0.13690	
	5		151.17		151.63	4.73	0.13611	

	N	q	α_0	α_1	α_2	α_3	α_4	
Method 4	2	4	151.70	4.73	0.13069	0.00866	0.00027	(c)
	3		151.63	4.73	0.13296	0.00883	0.00023	
	4		151.63	4.73	0.13291	0.00886	0.00023	
	5		151.63	4.73	0.13295	0.00887	0.00022	

5. References

1. Atkinson, C. Stress Singularities and Fracture Mechanics, Applied Mechs. Reviews, 32, 123-135 (1979)

2. Rizzo, F.J., An integral equation approach to boundary value problems of classical elastostatics, Quart. Appl. Math. 25, 83-95 (1967).

3. Cruse, T.A., Boundary integral equation method for three dimensional elastic fracture mechanics analysis. Air Force Office of Scientific Research TR-75-0813 (1975).

4. Cruse, T.A., Elastic Singularity Analysis, 1st Canadian Symposium on Innovative Numerical Analysis in Applied Engineering Science, Versailles (France) (1977)

5. Cruse, T.A., Two dimensional B.I.E. Fracture mechanics analysis, Appl. Math. Modelling 2, 287-293 (1978).

6. Williams, M.L., On the stress distribution at the base of a stationary crack, J. Appl. Mech. 24, 109-114 (1957).

7. Rice, J.R., Elastic Plastic fracture mechanics, in The Mechanics of Fracture, AMD 19, 23-53 (1978) ed. F. Erdogan.

8. Bilby, B.A., and Swinden, K.H., Plasticity at notches by linear dislocation arrays, Proc. Roy. Soc. (London) Ser A 285, 23-33 (1965).

9. Atkinson, C. and Kay, T.R., A simple model of relaxation at a crack tip, Acta Met., 679-685 (1971).

10. Atkinson, C. and Kanninen, M.F., A simple representation of crack tip plasticity: The inclined strip yield superdislocation model, Int. J. Frac. 13, 151-163 (1977).

11. Rice, J.R., A path independent integral and the approximate analysis of strain concentration by notches and cracks, J. Appl. Mech. 35, 379-386 (1968).

12. Eshelby, J.D., The force on an elastic singularity, Phil. Trans. Roy. Soc. A 244, 87-112 (1951).

13. Eshelby, J.D. "Energy relations and the energy-momentum tensor in continuum mechanics. in Inelastic Behavior of Solids (1970) 77-115 (ed. M.F. Kanninen et al.) McGraw-Hill, New York.

14. Knowles, J.K. and Sternberg, E. "On a class of conservation laws in linearised and finite elastostatics" Arch. Rat. Mech. Anal. 44, 187-211 (1972).

15. Gunther, W. Über einige Randintegrale der Elastomechanik, Abh. Braunschw. wiss. Ges. 14, 54-63, (1962).

16. Atkinson, C. A note on some crack problems in a variable modulus strip. 27, 639-647 (1975).

17. Eringen, A.C. Theory of Micropolar Elasticity, Ch. 7 of Fracture, Vol. 2 (1968), ed. Liebowitz (1968).

18. Atkinson, C. and Leppington, F.G., "The effect of couple stresses on the tip of a crack". Int. J. Solids Structures 13, 1103-1122 (1977).

19. Atkinson, C. and Smelser, R.E., Invariant integrals of thermo viscoelasticity. To appear in Int. J. Solids Structure.

20. Stern, M., Becher, E.B. and Dunham, R.S., A contour integral computation of mixed-mode stress intensity factors. Int. J. Frac. 12 (1976) 359-368.

21. Soni, M.L. and Stern, M., On the computation of stress intensity factors in fiber composite media using a contour integral method, Int. J. Frac. 12, 331-344 (1976)

22. Hong, C-C. and Stern, M., The computation of stress intensity factors in dissimilar materials, J. Elasticity 8 (1978) 21-34.

23. Stern, M. and Soni, M.L., On the computation of stress intensities at fixed-free corners. Int. J. Solids Structures (1976) 331-337.

24. Stern, M., The numerical calculation of thermally induced stress intensity factors, J. Elasticity 9 (1979) 91-95.

25. Cruse, T.A. and Van Buren, W., Three dimensional elastic stress analysis of a fracture specimen with an edge crack, Intl. Jnl. of Fracture Mechs. 7, 1-15 (1971).

26. Rizzo, F.J. and Shippy, D.J., A formulation and solution procedure for the general non-homogeneous elastic inclusion problem. Int. J. Solids Struct. 4, 1161-1173 (1968).

27. Snyder, M.D. and Cruse, T.A., Boundary-integral equation analysis of cracked anisotropic plates, Intl. Jnl. of Fracture, 11, 315-328 (1975).

28. Stroh, A.N., Dislocations and cracks in anisotropic elasticity, Phil. Mag. 3, 625-646 (1958).

29. Atkinson, C., The interaction between a dislocation and a crack, Int. J. Fracture Mechs, 2, 567-575 (1966).

30. Sinclair, J.E. and Hirth, J.P., Two dimensional elastic Green functions for a cracked anisotropic body, J. Physics, F, 5, 236-246 (1975).

31. Clements, D.L. and King, G.W., A method for the numerical solution of problems governed by elliptic systems in the cut plane, J. Inst. Maths. Applics. 24, 81-93 (1979).

32. Bilby, B.A. and Eshelby, J.D., Dislocations and the theory of Fracture, in Fracture, Vol. 1, 99-181 (1969) (ed. H. Liebowitz). Academic Press, (New York).

33. Atkinson, C., On dislocation pile ups and cracks in inhomogeneous media, Int. J. Engng. Sci., 10, 45-71 (1972).

34. Cook, T.S. and Erdogan, F., Stresses in bonded materials with a crack perpendicular to the interface, Int. J. Engng. Sci. 11, 745-766 (1972).

35. Rudolph, T.J. and Ashbaugh, N.E., An integral equation solution for a bounded elastic body containing a crack: Mode I deformation. Int. Jour. of Fracture 14, (1978) 527-541.

36. Chang, S.J. and Morgan, R.B., A boundary integral equation method for fracture problems with mixed mode deformations, ORNL/CSD-57 (June 1980).

37. Burgers, J.M., Proc. K. Ned. Akad. Wet. 42, 378-387 (1939)

38. Nabarro, F.R.N., Theory of Crystal Dislocations, (Oxford) (1967) (p.63).

39. Weaver, J., Three-dimensional crack analysis, Int. J. Solids Structs. 13, 321-330, 1977.

40. Montulli, L.T., The development and solution of boundary integral equations for crack problems in fracture mechanics, Ph.D. Thesis U.C.L.A. (1975).

41. Xanthis, L.S. Private Communication.

42. Barone, M.R. and Robinson, A.R., Determination of elastic stresses at notches and corners by integral equations, Int. J. Solids Structures, 8, 1319-1338 (1972).

43. Xanthis, L.S., Bernal, M.J.M. and Atkinson, C., The treatment of singularities in the calculation of stress intensity factors using the boundary integral equation method, Comp. Methods in Appl. Mechs. and Engng, 26, 285-304 (1981).

44. Lachat, J.C., 'A further development of the boundary integral technique for elastostatics' (p.80). Ph.D. Thesis, University of Southampton (1975).

45. Lachat, J.C. and Watson, J.O., A second generation B.I.E. program for 3-dimensional elastic analysis, B.I.E. Method: Computational Applications in Applied Mechanics ASME (1975).

46. Kondrat'ev, V.A. Boundary problems for elliptic equations in domains with conical or angular points, Trans. Moscow Math. Soc. (1967) 227-313.

47. Papamichael, N. and Whiteman, J.R. A numerical conformal transformation method for harmonic mixed boundary value problems in polygonal domains. Z. angew. Math. Phys. 24 (1973) 304-316.

48. Morley, L.S.D. Finite element solution of boundary-value problems with non-removable singularities. Phil. Trans. Roy. Soc. London A 275 (1973) 463-488.

49. Barsoum, R.S. On the isoparametric finite elements in linear fracture mechanics, Internat. J. Numer. Meths. Engrg. 10 (1976) 25-37.

50. Henshell, R.D. and Shaw, K.G. Crack tip finite elements are unnecessary, Internat. J. Numer. Meths. Engrg. 9 (1975) 495-507.

51. Lynn, P.P. and Ingraffea, A.R. Transition elements to be used with quarter-point crack-tip elements, Internat. J. Numer. Meths. Engrg. 6 (1978) 1031-1036.

52. Pu, S.L., Hussain, M.A. and Lorensen, W.E. The collapsed cubic isoparametric elements as a singular element for crack problems, Internat. J. Numer. Meths. Engrg. 12 (1978) 1727-1742.

53. Bernal, M.J.M. and Xanthis, L.S. Transition elements to be used with parametric cubic geometry crack tip elements, to appear.

54. Symm, G.T. Treatment of singularities in the solution of Laplace's equation by an integral equation method, NPL Report NAC (31 January 1973).

55. Papamichael, N. and Symm, G.T. Numerical techniques for two-dimensional Laplacian problems, Comput. Meths. Appl. Mech. Engrg. 6 (1975) 175-194.

56. Schatz, A.H. and Wahlbin, L.B. Maximum norm estimates in the finite element method on plane polygonal domains, part I. Math. Comput. 32 (1978) 73-109.

57. Atkinson, C., Xanthis, L.S. and Bernal, M.J.M., Boundary integral equation crack-tip analysis and applications to elastic media with spatially varying elastic properties, Comp. Methods in Appl. Mechs. and Engng., (1982) (To appear).

FIGURE CAPTIONS

Figure 1: Definition of crack modelling terms used in deriving equation (.16) (After Cruse [3,4,5])

Figure 2: Typical crack tip co-ordinate system

Figure 3: Fracture modes. 3(a) opening mode; 3(b) sliding mode; 3(c) anti-plane shearing mode

Figure 4: Contours for integrals around crack tip

Figure 5: A crack positioned symmetrically in a body

Figure 6: A crack positioned unsymmetrically in a body

Figure 7: A Somigliana dislocation

Figure 8: Numbering of elements and nodes : case p = 4

Figure 9: An interelement corner node

Figure 10: Square region with a slit

Figure 11: (a) Element numbering for the model problem
(b) Notation used in modelling t ahead of the crack
(c) Illustration of singular and first (compatible) continuation Lagrangian 'square-root' elements

Figure 12: Notation used in modelling u on the crack

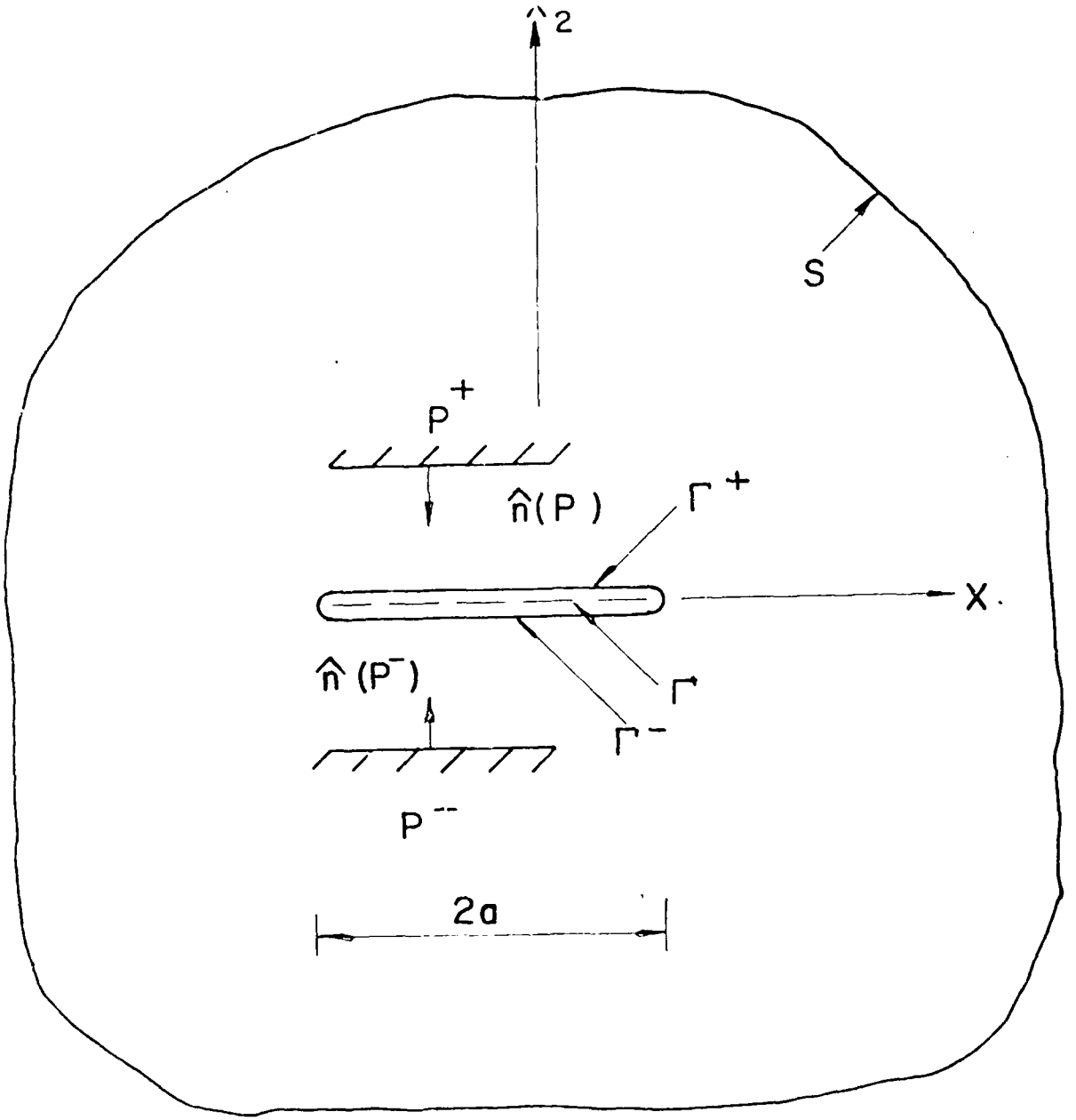

FIG. 1

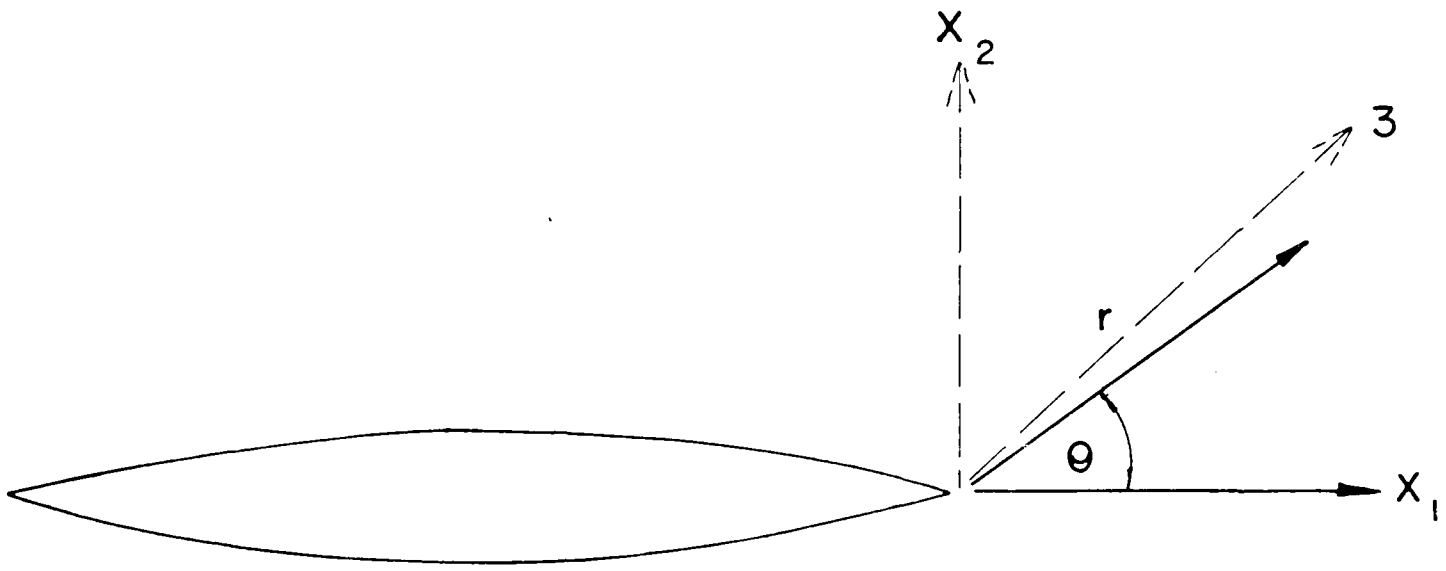

FIG. 2.

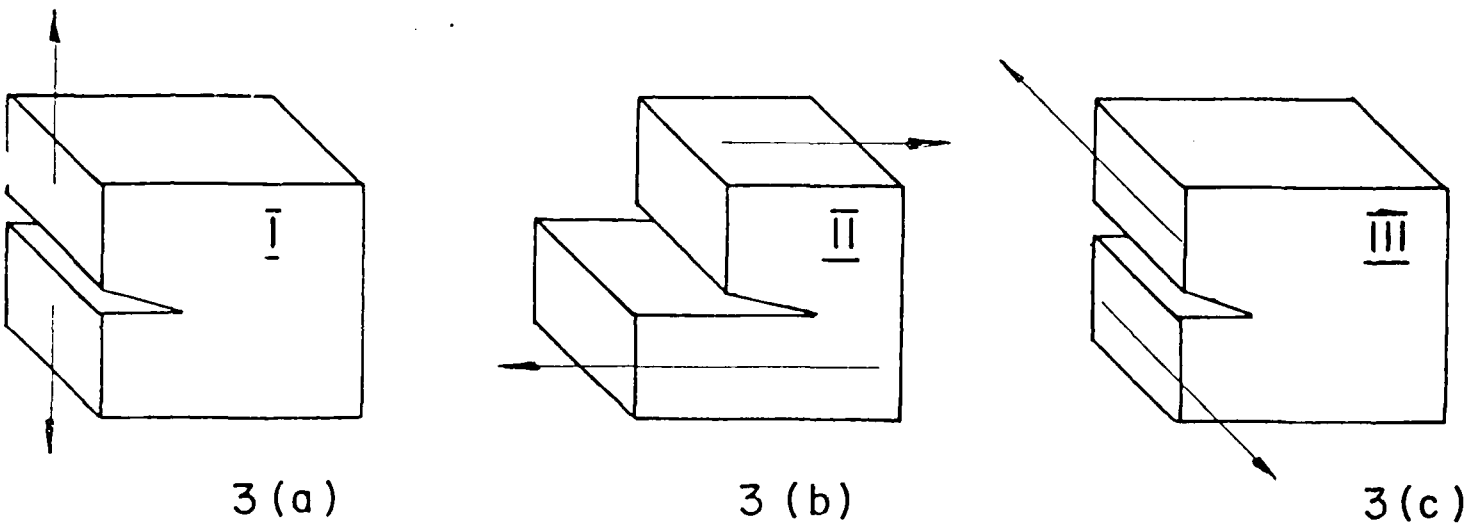

3 (a) 3 (b) 3 (c)

FIG 3

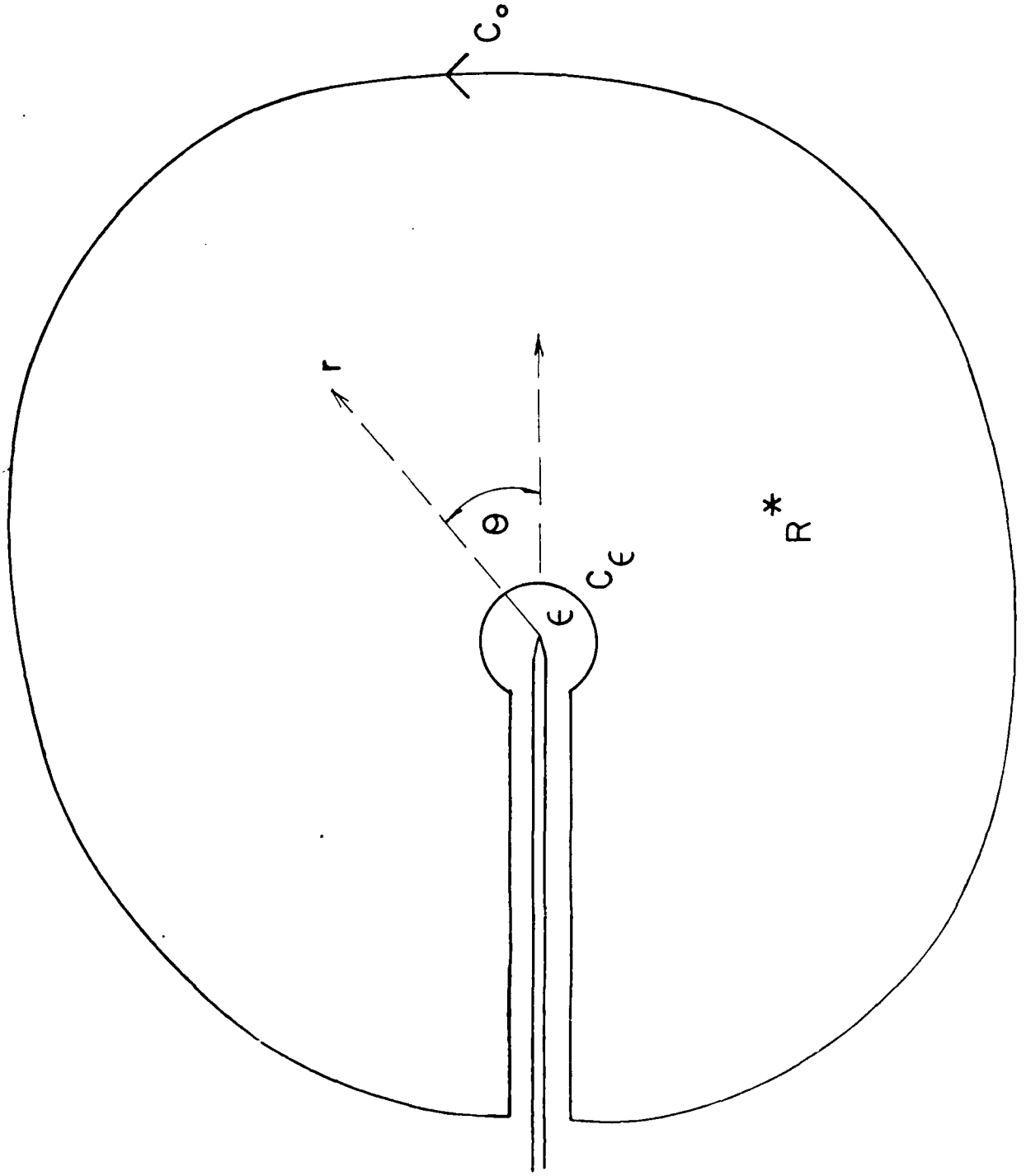

FIG 4

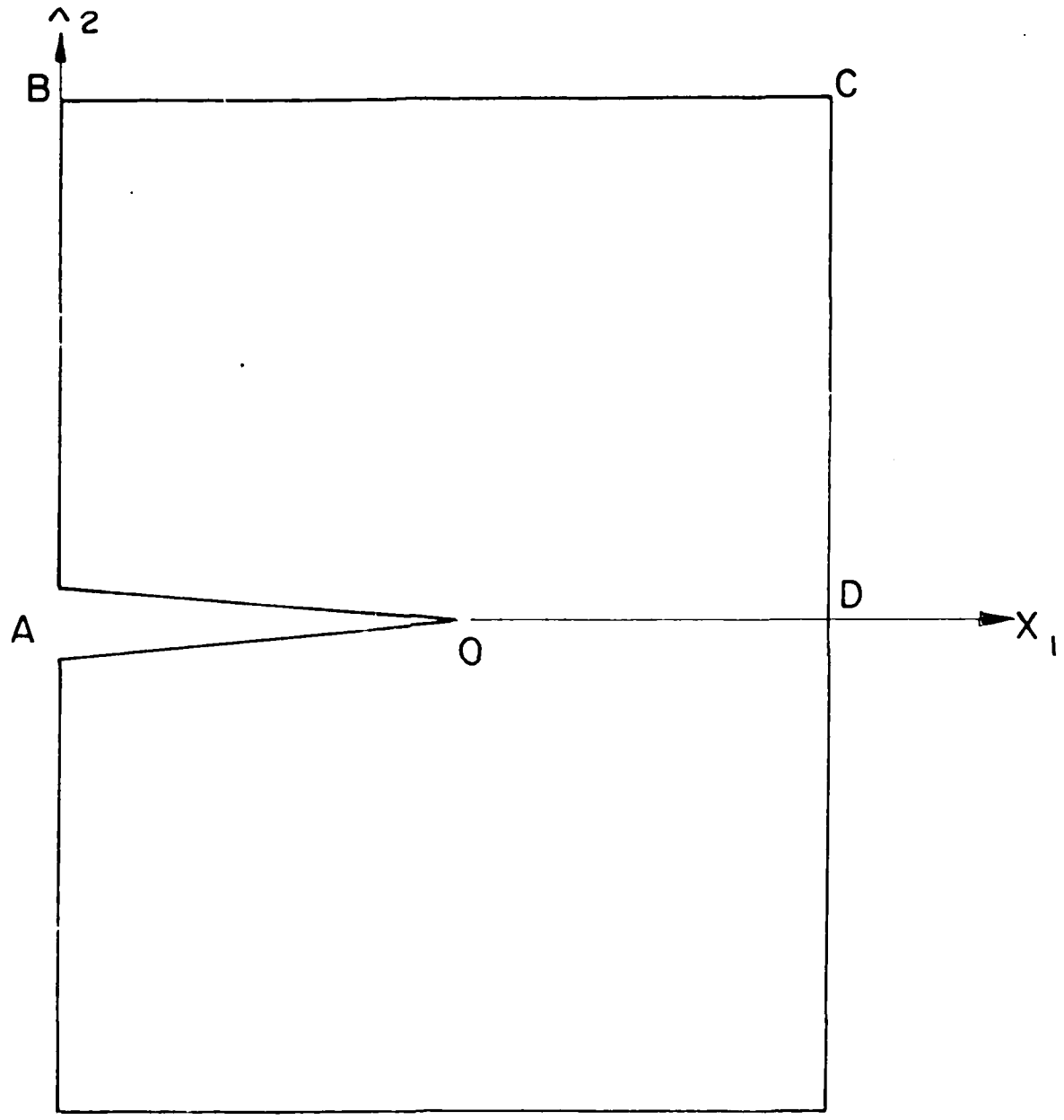

FIG. 5

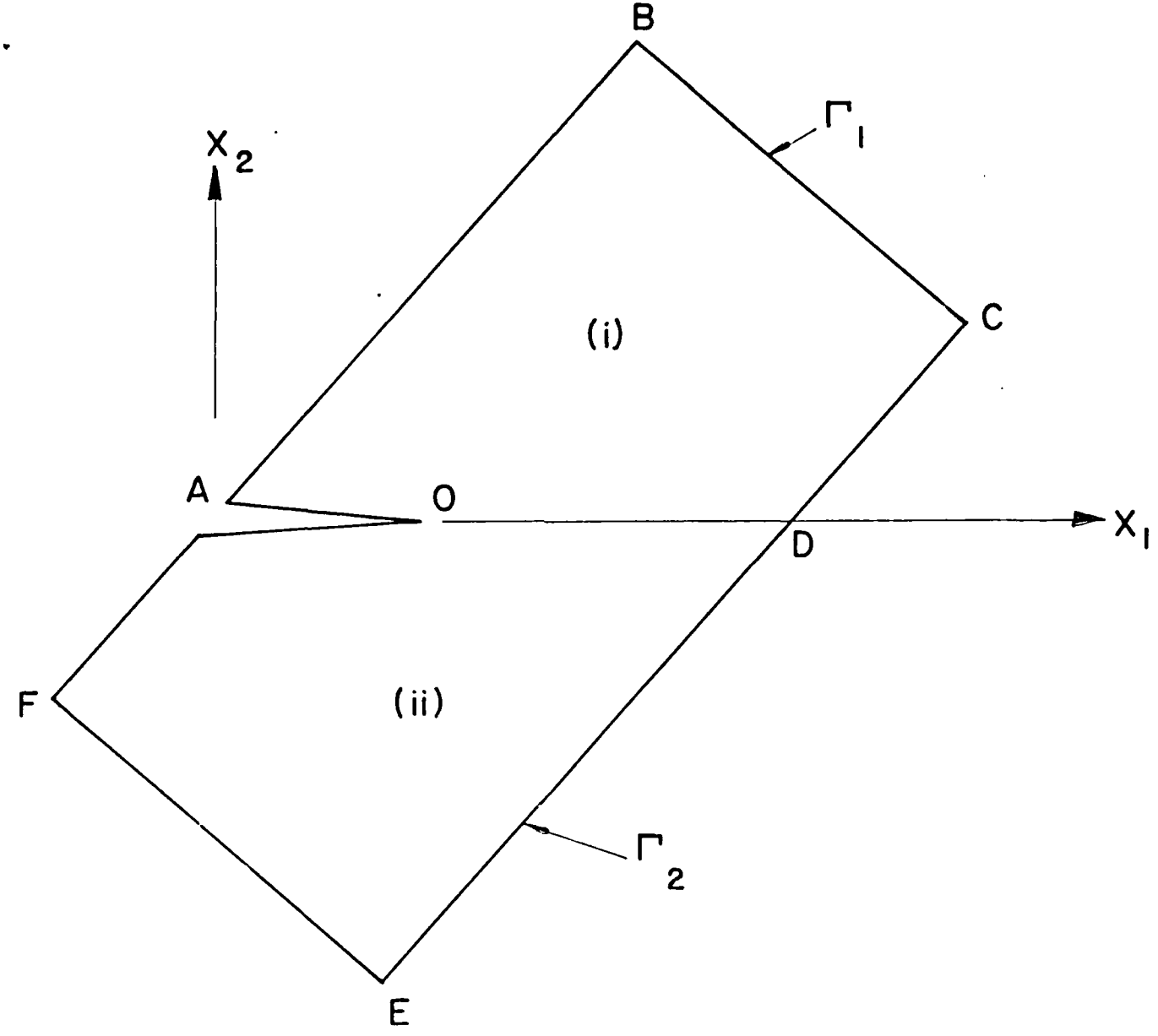

FIG 6

FIG 7

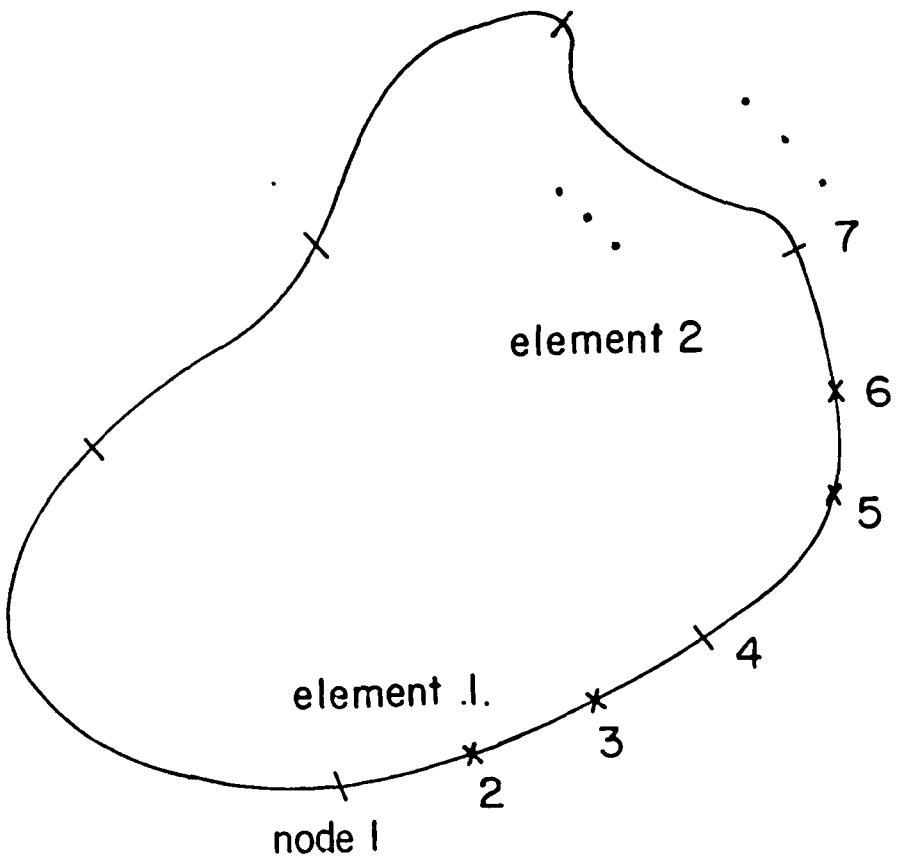

FIG.8.

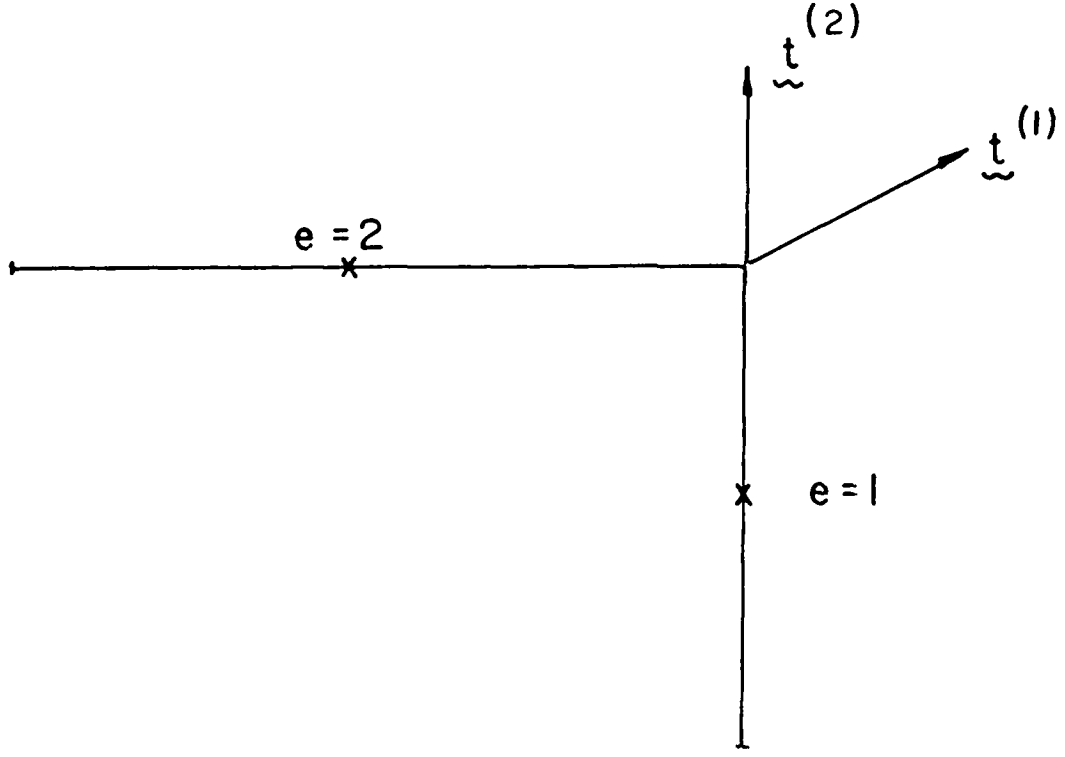

FIG 9

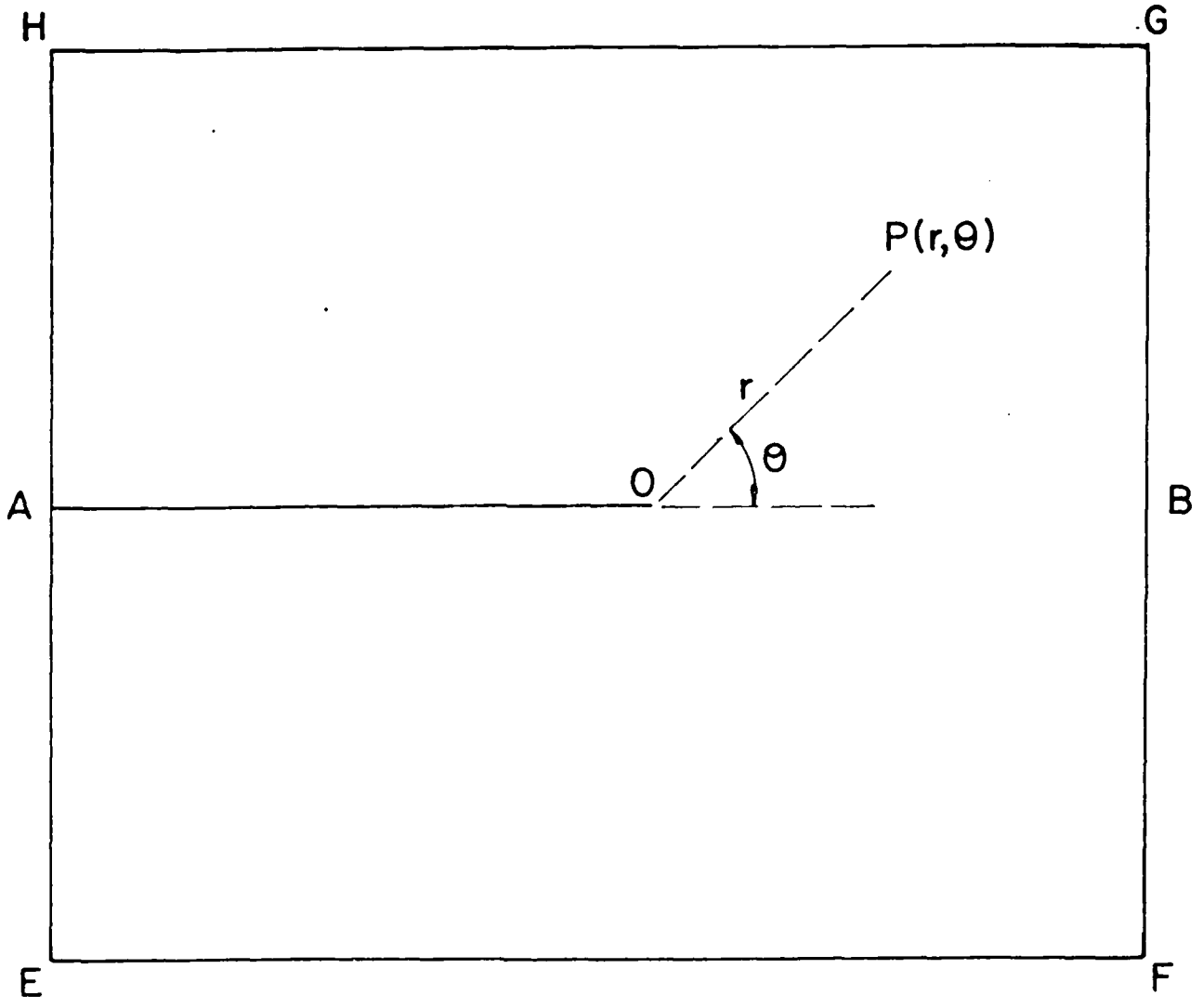

FIG .10.

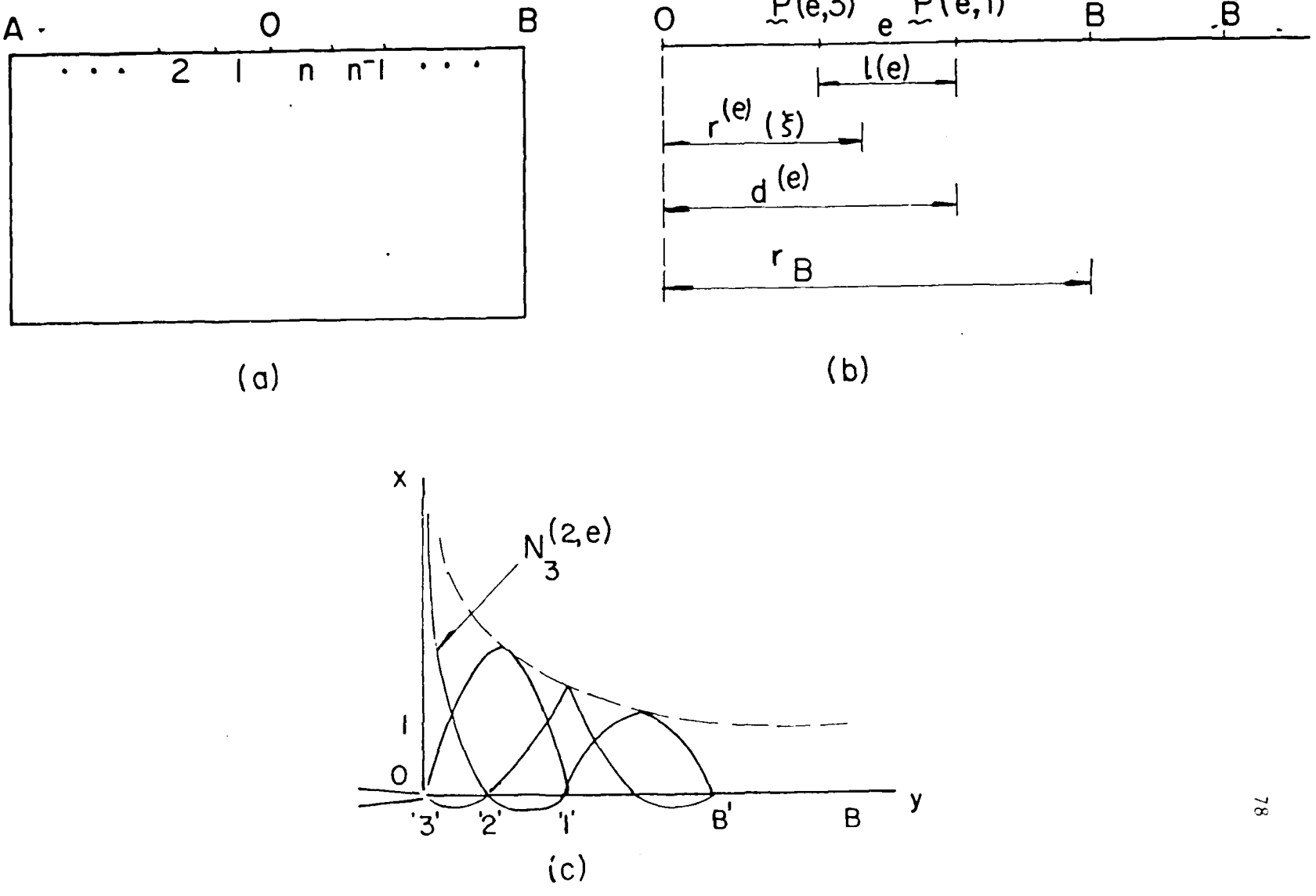

78

FIG 11

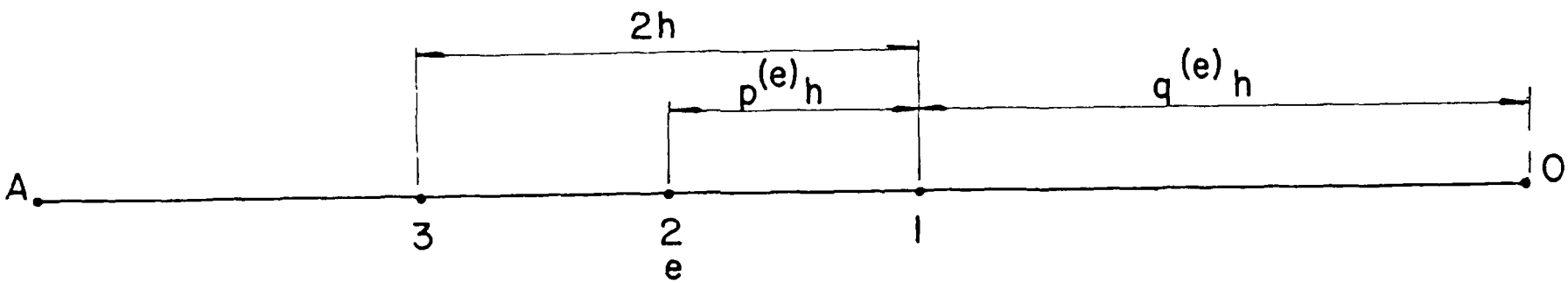

FIG 12

END

FILMED

2-85

DTIC